Intravenous Bacille Calmette–Guérin vaccination protects simian immunodeficiency virus-infected macaques from tuberculosis

Erica C. Larson [1,2] ✉, Amy L. Ellis-Connell[3], Mark A. Rodgers [1], Abigail K. Gubernat[1], Janelle L. Gleim[1], Ryan V. Moriarty [3], Alexis J. Balgeman[3], Cassaundra L. Ameel[1], Solomon Jauro[1], Jaime A. Tomko[1], Kara B. Kracinovsky[1], Pauline Maiello [1], H. Jake Borish[1], Alexander G. White[1], Edwin Klein[4], Allison N. Bucsan[5], Patricia A. Darrah[5], Robert A. Seder [5], Mario Roederer[5], Philana Ling Lin[6], JoAnne L. Flynn [1,2], Shelby L. O'Connor [3,7] & Charles A. Scanga [1,2]

Tuberculosis, caused by *Mycobacterium tuberculosis* (Mtb), is the most common cause of death in people living with human immunodeficiency virus (HIV). Intra-dermal Bacille Calmette–Guérin (BCG) delivery is the only licensed vaccine against tuberculosis; however, it offers little protection from pulmonary tuberculosis in adults and is contraindicated in people living with HIV. Intravenous BCG confers protection against Mtb infection in rhesus macaques; we hypothesized that it might prevent tuberculosis in simian immunodeficiency virus (SIV)-infected macaques, a model for HIV infection. Here intravenous BCG-elicited robust airway T cell influx and elevated plasma and airway antibody titres in both SIV-infected and naive animals. Following Mtb challenge, all 7 vaccinated SIV-naive and 9 out of 12 vaccinated SIV-infected animals were protected, without any culturable bacteria detected from tissues. Peripheral blood mononuclear cell responses post-challenge indicated early clearance of Mtb in vaccinated animals, regardless of SIV infection. These data support that intravenous BCG is immunogenic and efficacious in SIV-infected animals.

Mycobacterium tuberculosis (Mtb) infection results in over ten million cases of active tuberculosis (TB) worldwide every year[1]. People living with human immunodeficiency virus (PLWHIV) are very susceptible to Mtb infection and TB disease[2]. TB rapidly progresses and accounts for one in every three deaths among PLWHIV[3]. Although TB is treatable, complications in PLWHIV such as drug–drug interactions with anti-retroviral therapy (ART), issues with compliance due to adverse drug effects, access to healthcare and development of TB–immune

[1]Department of Microbiology and Molecular Genetics, School of Medicine, University of Pittsburgh, Pittsburgh, PA, USA. [2]Center for Vaccine Research, School of Medicine, University of Pittsburgh, Pittsburgh, PA, USA. [3]Department of Pathology and Laboratory Medicine, University of Wisconsin, Madison, WI, USA. [4]Division of Laboratory Animal Resources, School of Medicine, University of Pittsburgh, Pittsburgh, PA, USA. [5]Vaccine Research Center, National Institute of Allergy and Infectious Diseases, National Institutes of Health, Bethesda, MD, USA. [6]Department of Pediatrics, Children's Hospital of Pittsburgh, School of Medicine, University of Pittsburgh, Pittsburgh, PA, USA. [7]Wisconsin National Primate Research Center, University of Wisconsin, Madison, WI, USA. ✉e-mail: erl72@pitt.edu

reconstitution inflammatory syndrome remain a barrier to successful TB treatment in this vulnerable population. Vaccines are the best public health approach to prevent infectious diseases such as TB, especially in resource-poor settings. However, safety, immunogenicity and efficacy are a concern in PLWHIV due to immunosuppression from chronic HIV infection.

Bacille Calmette–Guérin (BCG) is the only vaccine currently licensed for TB prevention. BCG is a live attenuated *Mycobacterium bovis* strain delivered intra-dermally at birth. It confers excellent protection against disseminated TB in children (for example, meningeal TB and extrapulmonary TB)[4]; however, BCG provides little protection against transmissible pulmonary TB in adolescents and adults, suggesting waning efficacy[5]. The implementation of BCG as a vaccine has remained largely unchanged since its discovery over 100 years ago, and it continues to be one of the most widely used vaccines in the world. There is a critical need to improve vaccine efficacy against pulmonary TB in adolescents and adults. However, BCG is contraindicated in people who are immunosuppressed, such as PLWHIV[6]. The exception to this contraindication is HIV-infected individuals who are receiving ART, are clinically well and have a CD4 T cell count of >200 cells mm^{-3} (ref. 7). It is imperative that vaccines are developed that are not only safe and effective for immunocompetent individuals, but also protect susceptible populations[4].

Several groups have investigated different ways to boost protection conferred by BCG, such as subunit vaccines, co-administration with adenoviral vectors encoding Mtb proteins, and use of recombinant strains of BCG[8–11]. However, these efforts were unsuccessful at achieving robust or sterilizing immunity. Studies in mice[12] and non-human primates (NHP)[13] showed that concurrent infection with Mtb confers protection from a secondary Mtb challenge, suggesting that high-level protection against Mtb is possible. Recently, substantial protection against TB has been achieved in macaque models of TB using several approaches including cytomegalovirus-vectored delivery of TB antigens[14] and mucosal delivery of BCG[15]. Recent work by our group and others demonstrated that intravenous (IV) BCG immunization confers robust protection against TB in rhesus macaques[16–19]. Notably, IV delivery of BCG protected nine out of ten macaques from TB disease (<100 Mtb colony-forming units (CFU)), with six out of ten animals exhibiting sterilizing immunity (undetectable CFU)[16]. IV BCG-elicited protection was associated with high levels of mycobacteria-specific T cells in airways, tissue-resident memory T cells[16] and robust immunoglobulin (Ig) M responses[20].

While the above studies in immunocompetent macaques generated renewed enthusiasm for TB vaccines, these vaccines have not been evaluated in the setting of immune suppression, such as simian immunodeficiency virus (SIV) infection. Modelling PLWHIV merits special consideration especially for live attenuated vaccines such as BCG. It remains unknown whether IV delivery of BCG is safe and immunogenic in SIV-infected NHP, and whether the robust protection conferred by IV BCG in healthy animals would be recapitulated in immunocompromised macaques.

In this Article, we extended the studies of Darrah et al.[16] to determine whether IV BCG immunization is safe, immunogenic and protective in our established model of SIV/Mtb co-infection in Mauritian cynomolgus macaques (MCM). MCM have similar high susceptibility to Mtb infection and disease as rhesus macaques[21] and SIV infection exacerbates TB progression in this species[22]. We show that MCM chronically infected with SIV can be vaccinated with high-dose IV BCG without adverse effects. Furthermore, IV BCG elicits strong immune responses in both SIV-infected and SIV-naive macaques. MCM responses were consistent with those reported in rhesus macaques[16], including the induction of T cells in the airways as well as robust antibody responses in blood and airways. Most strikingly, IV BCG conferred robust protection against Mtb challenge irrespective of SIV infection status–providing sterilizing immunity in all 7 SIV-naive animals and 9 out of 12 SIV-infected animals.

Results

IV BCG is safe in SIV-infected animals

We sought to determine whether IV BCG was safe, immunogenic and efficacious in animals with a pre-existing, chronic SIV infection using our established model of SIV/Mtb co-infection in MCM[22,23]. This study included four groups of animals: SIV-naive, unvaccinated (Unvax) ($N = 8$); SIV-naive, vaccinated (IV BCG) ($N = 7$); SIV+, unvaccinated (SIV/Unvax) ($N = 4$; historical controls included for TB outcome only, $N = 7$); and SIV+, vaccinated (SIV/IV BCG) ($N = 12$) (Extended Data Fig. 1a). For the SIV+ groups, animals were intrarectally infected with SIVmac239 (3,000 50% tissue culture infectious dose). Five months later, some animals were vaccinated intravenously with BCG at 8×10^7 CFU. Due to concerns over potential disseminated BCG disease in immunocompromised animals, animals were treated with an 8-week regimen of isoniazid/rifampin/ethambutol (HRE) 3–4 weeks after IV BCG vaccination. Unvaccinated animals also received HRE to minimize any confounding effects due to antibiotic therapy. Four weeks after antibiotic cessation (4 months post-BCG in vaccinated animals), all animals were challenged with low-dose Mtb Erdman (~11 CFU) via bronchoscope, followed for 3 months and then necropsied.

To assess the safety of IV BCG, blood cultures were performed 2 weeks after vaccination, and erythrocyte sedimentation rate (ESR), an indicator of inflammation, and weight were measured over the course of vaccination. A total of 4 out of the 7 SIV-naive, vaccinated animals, and 1 out of the 12 SIV+ vaccinated animals, had culturable BCG in their blood 2 weeks after vaccination (Extended Data Fig. 1b). One animal in the SIV+ vaccinated group had a transiently increased ESR ~1 month post-vaccination (Extended Data Fig. 1c). There were no notable changes in clinical status, ESR or weight in the remainder of the animals following vaccination (Extended Data Fig. 1c,d). Thus, based on these clinical measures, IV BCG appears to be safe in SIV+ macaques, at least when treated with HRE within 3–4 weeks after administration.

It is worth noting that two IV BCG-vaccinated animals did not reach Mtb challenge, probably due to reasons unrelated to BCG. The first animal, 192-18, was SIV-naive and died 12 weeks after vaccination due to a presumed fatal arrhythmia during bronchoalveolar lavage (BAL) with no history of weight loss or elevated ESR (Extended Data Fig. 2a,b). The second, 82-18, was SIV-infected and had persistently high plasma viraemia (Extended Data Fig. 2c). Following IV BCG, it exhibited weight loss and elevated ESR (Extended Data Fig. 2d,e). Rapid clinical deterioration ~12 weeks after vaccination led to euthanasia and necropsy where a large abdominal lymphoma was identified (Extended Data Fig. 2f). Neither animal had detectable BCG by blood culture 2 weeks after vaccination, and 82-18 showed no histopathological signs of granulomatous disease. Data from these animals were excluded from further analysis.

IV BCG triggers a transient burst of SIV replication

Plasma viraemia was assessed serially in vaccinated and unvaccinated SIV+ animals. All animals in this study had at least one copy of the major histocompatibility complex (MHC) haplotype M1. This ensures all animals shared at least one copy of the MHC alleles of the M1 haplotype, so that all animals should mount a population of mycobacterial-specific T cells targeting the same epitopes[24]. As previously reported[25], M1+ animals display either spontaneously controlled viraemia (<10^4 copies ml^{-1}) or high levels of viraemia (>10^5 copies ml^{-1}). As expected, plasma viraemia peaked 1–2 weeks post SIV infection and by 7–8 weeks post-infection, animals showed a range of viral set points. There was a spike in plasma viraemia ~2 weeks following BCG vaccination (Fig. 1a). This increase in plasma viraemia was significant in SIV+ vaccinated animals compared with time-matched SIV+ unvaccinated animals (Fig. 1b). Plasma viraemia in SIV+ vaccinated animals returned to their pre-vaccination levels during HRE treatment, before Mtb challenge (Fig. 1b). Following Mtb challenge, we did not observe a consistent effect on plasma viraemia as reported previously[22]. These data indicate that IV BCG was a potent stimulator of viral replication; however, this effect was transient.
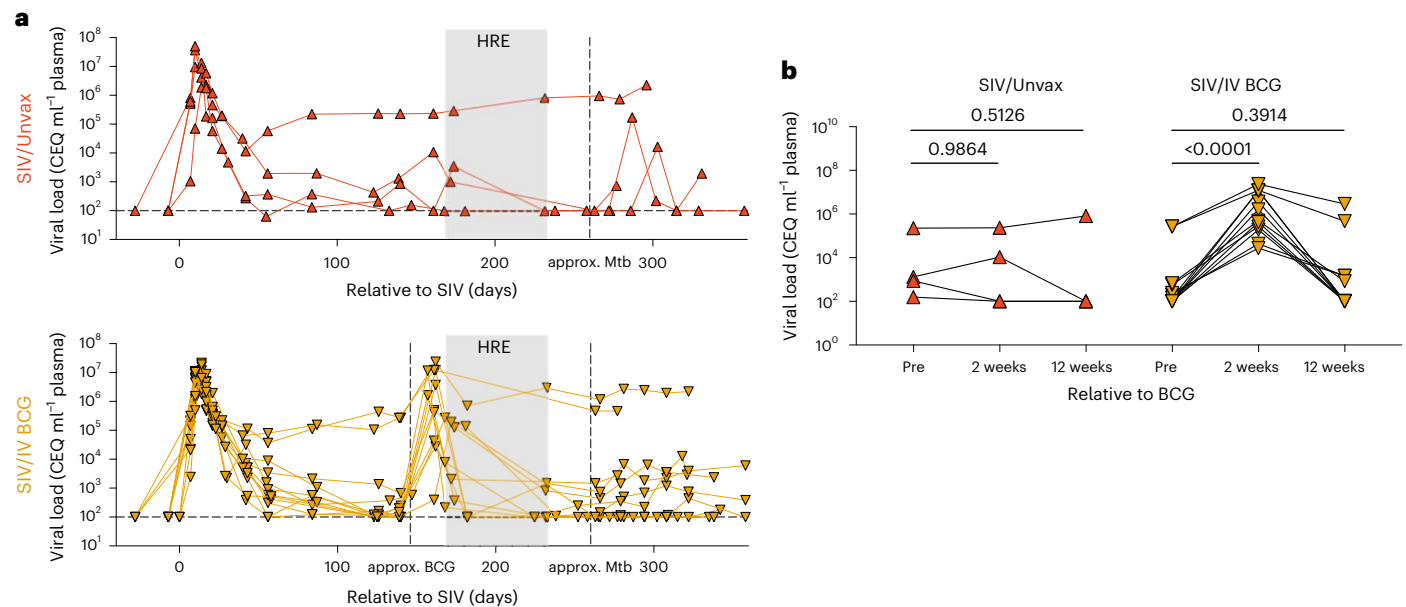
Fig. 1 | Plasma viraemia of SIV+ unvaccinated and vaccinated animals. Plasma viral copy equivalents were determined by qRT–PCR. Each point indicates an individual animal (SIV/Unvax, $n = 4$; SIV/IV BCG, $n = 12$). **a**, Plasma viral load (in copy equivalents (CEQ) ml^{−1}) of SIV+ unvaccinated (top, red up-pointing triangles) and SIV+ vaccinated (bottom, gold down-pointing triangles) animals over the course of the study. Horizontal dashed line represents the limit of detection.

b, Plasma viral load of each group before (pre), 2 weeks and 12 weeks, relative to BCG vaccination. Time-matched plasma from SIV+ unvaccinated animals served as a control. Repeated measure one-way ANOVAs were performed on each group (SIV/Unvax, $P = 0.5759$; SIV/IV BCG, $P < 0.0001$). Multiple comparisons relative to 'pre-BCG' were performed using Dunnett's multiple comparisons tests. Adjusted P values for multiple comparisons are shown.

IV BCG induces mycobacterial-specific T cell airway influx

Since the primary site of Mtb infection is the lung, we assessed whether IV BCG vaccination led to enhanced immune responses in airways of SIV+ and SIV-naive MCM as previously described in SIV-naive rhesus macaques[16]. Flow cytometry on serial BAL showed a striking influx of T cells into the airways 4 weeks after IV BCG in both SIV-naive and SIV+ animals (Fig. 2a). This high number of T cells was sustained 12 weeks after vaccination (1 month before Mtb challenge), regardless of SIV status. There was also a significant influx of B cells and natural killer (NK) cells in both vaccinated groups (Fig. 2a). Mucosal-associated invariant T (MAIT) cells, Vγ9+ γδ T cells, CD4+ T cells and CD8+ T cells significantly increased in number following vaccination and were maintained 12 weeks after vaccination, just before Mtb challenge (Fig. 2b).

Next, we assessed whether the T cells present in the airways of vaccinated animals were able to produce cytokines associated with Mtb control (interferon gamma (IFNγ), tumour necrosis factor (TNF), interleukin-2 (IL-2)[26–28] in response to mycobacterial-specific antigens (purified protein derivative (PPD)). There was a significant increase in the number of cytokine-producing CD4+ T cells, reaching 10^4–10^6 cells, in the airways of SIV-naive and SIV+ vaccinated animals at 4 and 12 weeks after vaccination (Fig. 2c). Cytokine-producing CD8+ T cells were significantly elevated, albeit lower than the CD4+ T cells, following vaccination in both BCG-vaccinated groups (Fig. 2c). There were increased numbers of mycobacterial-responsive CD4+ T cells producing IL-17A, a cytokine associated with mucosal immunity[29], in the airways of both SIV-naive and SIV+ macaques following vaccination (Fig. 2d). Mycobacterial-responsive CD8+ T cells producing IL-17A was very low in both groups (Fig. 2d). Together, these data indicate that IV BCG vaccination induces a rapid and sustained influx of mycobacterial-specific T cells into the airways, regardless of SIV status.

IV BCG induces mycobacterial-specific responses in blood

We assessed the circulating immune cell landscape and T cell responses to mycobacterial and Mtb-specific stimuli in peripheral blood mononuclear cells (PBMC). There was a modest but significant increase in the frequency of T cells, along with a small decline in B cell, NK cell and plasmacytoid dendritic cell populations, following BCG vaccination at 4 weeks (Fig. 3a). The frequency of MAIT cells significantly increased 4 weeks after vaccination and was maintained 12 weeks after vaccination, regardless of SIV status (Fig. 3b). Vγ9+ γδ T cells significantly increased 4 weeks after BCG vaccination in both vaccinated groups (Fig. 3b). However, SIV+ animals had significantly higher frequencies of Vγ9+ γδ T cells compared with SIV-naive animals (Fig. 3b). Vγ9+ γδ T cell frequencies returned to pre-infection levels by 12 weeks post-BCG. The frequency of CD4+ T cells did not change significantly over vaccination (Fig. 3b), although CD4+ T cell frequencies were significantly lower in SIV+ compared with SIV-naive animals 4 weeks after IV BCG (Fig. 3b), most probably due to the transient spike in SIV replication[30]. CD8+ T cells, on the other hand, significantly declined in both vaccinated groups 4 weeks after BCG vaccination (Fig. 3b). Frequencies of both CD4+ and CD8+ T cells returned to near pre-vaccination baseline levels by week 12 after IV BCG.

CCR5+ and CXCR3+CCR6+ CD4+ T cell frequencies peaked in PBMC 4 weeks after vaccination and remained elevated compared with pre-BCG regardless of SIV status (Extended Data Fig. 3a,b). CCR5 is expressed on effector T cells and is a co-receptor the facilitates HIV/SIV infection[31,32], whereas T cells expressing both CXCR3 and CCR6 are associated with T helper 1 (T_H1)/T_H17 (T_H1^*) responses[33,34]. In addition, the frequency of circulating CD4+ T follicular helper (T_{FH}) cells in SIV+ vaccinated animals were elevated across all timepoints, including pre-BCG, compared with SIV-naive animals, probably due to chronic SIV (Extended Data Fig. 3c). There was a small but significant reduction in CD4+ T regulatory (T_{reg}) cells in both vaccinated groups 4 weeks after IV BCG (Extended Data Fig. 3d).

CD4+ and CD8+ T cells in blood produced cytokines (IFNγ, TNF and IL-2) and increased expression of CD154, a marker associated with antigen-specificity[35], upon stimulation to mycobacterial antigens (Mtb whole cell lysate (WCL)) at 4 and 12 weeks post-BCG (Fig. 4a, b), with no significant differences between SIV-naive and SIV+ macaques. Cytokine production by CD4+ T cells remained elevated in both groups
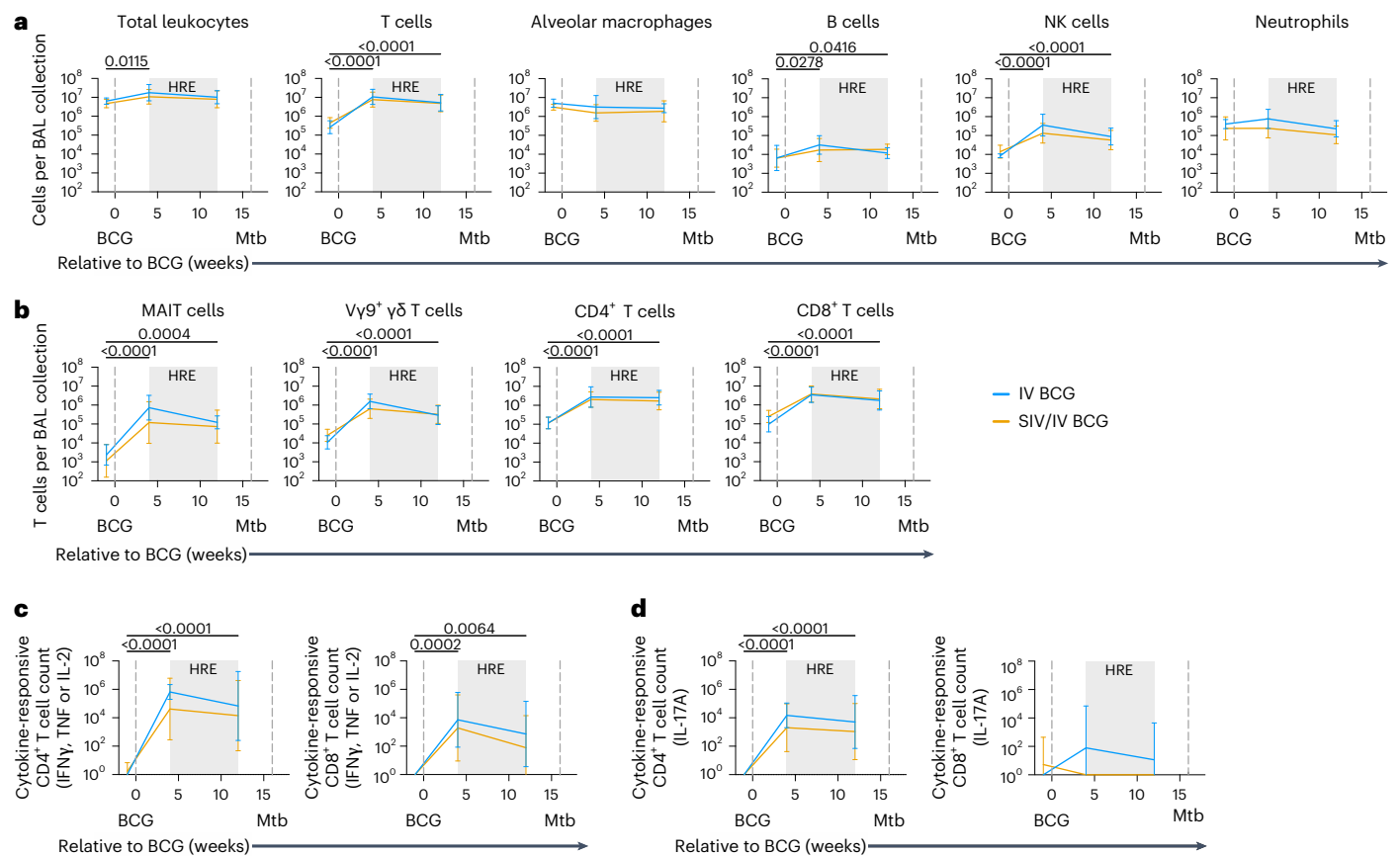
Fig. 2 | Leukocyte and T cell subsets and T cell response in BAL after BCG vaccination. a, Number of leukocytes per BAL collection. **b**, Number of T cell subset cells per BAL collection. **c**, Number of cytokine-responsive (IFNγ, TNF and IL-2) CD4+ and CD8+ T cells in BAL after 14 h stimulation with PPD. **d**, Number of IL-17A-responsive CD4+ and CD8+ T cells in BAL after 14 h stimulation with PPD. Data are mean and s.d. of SIV-naive (light blue) and SIV+ (gold) vaccinated animals (**a**–**d**). SIV-naive vaccinated animals: pre-BCG (*n* = 5), 4 weeks post-BCG (*n* = 6) and 12 weeks post-BCG (*n* = 6). SIV+ vaccinated animals: pre-BCG (*n* = 10), 4 weeks post-BCG (*n* = 11) and 12 weeks post-BCG (*n* = 8). Individual animal data are shown in Supplementary Data 5. Mixed effects models with subject as a random variable were used to assess mean differences among timepoints and vaccine groups. Timepoints were compared with 'pre-BCG' control using Dunnett's multiple comparison tests. No significant differences between vaccination groups were found. Significant *P* values (*P* < 0.05) across time are shown above each graph. Fixed effect test results and Dunnett's multiple comparisons are included in Supplementary Table 2a. All statistical tests were two-sided.

until 12 weeks post-Mtb challenge (Fig. 4a). However, following Mtb challenge, cytokine production in response to peptide pools of the Mtb-specific antigens early secreted antigenic target-6 (ESAT-6) and cyan fluorescent protein-10 (CFP-10) (antigens not present in BCG) by CD4+ T cells was only observed in non-vaccinated SIV-naive or SIV+ macaques (Fig. 4c,d). IFNγ ELISpot assays of PBMC collected pre- and post-Mtb challenge also showed that both unvaccinated groups generated an IFNγ response to Mtb-specific ESAT-6 and CFP-10 (Fig. 4e). Notably, PBMC from vaccinated animals, regardless of SIV status, did not generate an IFNγ response to Mtb antigens (Fig. 4e). These data suggest that IV BCG induces rapid and early clearance of Mtb, precluding a measurable T cell response (IFNγ, TNF or IL-2) to infection, as noted in our previously published study on IV BCG in SIV-naive rhesus macaques[16].

IV BCG induces mycobacterial-specific antibody responses

Recent studies have shown that humoral immunity may play role in the control of Mtb infection and is associated with protection by IV BCG[20,36–38]. Humoral responses to mycobacterial antigens (Mtb WCL) in plasma and BAL fluid (BALF) before and 12 weeks after IV BCG vaccination (4 weeks before Mtb challenge) were assessed by enzyme-linked immunosorbent assay (ELISA). There were significant increases in WCL-reactive IgG and IgA levels in the plasma and BALF of both SIV-naive and SIV+ animals following vaccination (Fig. 5a–d). WCL-reactive IgM in plasma increased after vaccination in SIV-naive but not in SIV+ animals (Fig. 5e). It is possible that we were unable to detect a change in plasma IgM in the SIV+ animals due to the high baseline IgM before IV BCG vaccination, which may be due to the inherent pentameric nature of IgM or presence of rheumatoid factor in plasma that contributes to high background levels[39–41]. Nevertheless, there was a significant increase in BALF IgM levels in both groups after IV BCG vaccination (Fig. 5f). Thus, IV BCG induces mycobacterial-specific humoral immune responses in both SIV-naive and SIV+ animals.

IV BCG protects SIV+ macaques from TB

A total of 4 months after BCG vaccination (1 month after HRE cessation), animals were challenged with low-dose Mtb Erdman via bronchoscope. Inflammation and progression of Mtb infection were serially quantified using ^{18}F-fluorodeoxyglucose (FDG) positron emission tomography–computed tomography (PET/CT) imaging. Total lung FDG activity, a surrogate for lung inflammation, revealed substantial lung inflammation in both unvaccinated groups as early as 4 weeks post-Mtb challenge, which remained elevated until necropsy (Fig. 6a). In contrast, SIV-naive vaccinated animals displayed minimal lung inflammation over the 12 weeks of Mtb infection (Fig. 6a). SIV+ vaccinated animals showed variable lung inflammation, especially at 8 weeks post-Mtb challenge (Fig. 6a). We previously showed that dissemination of granulomas, an indicator of TB disease progression,
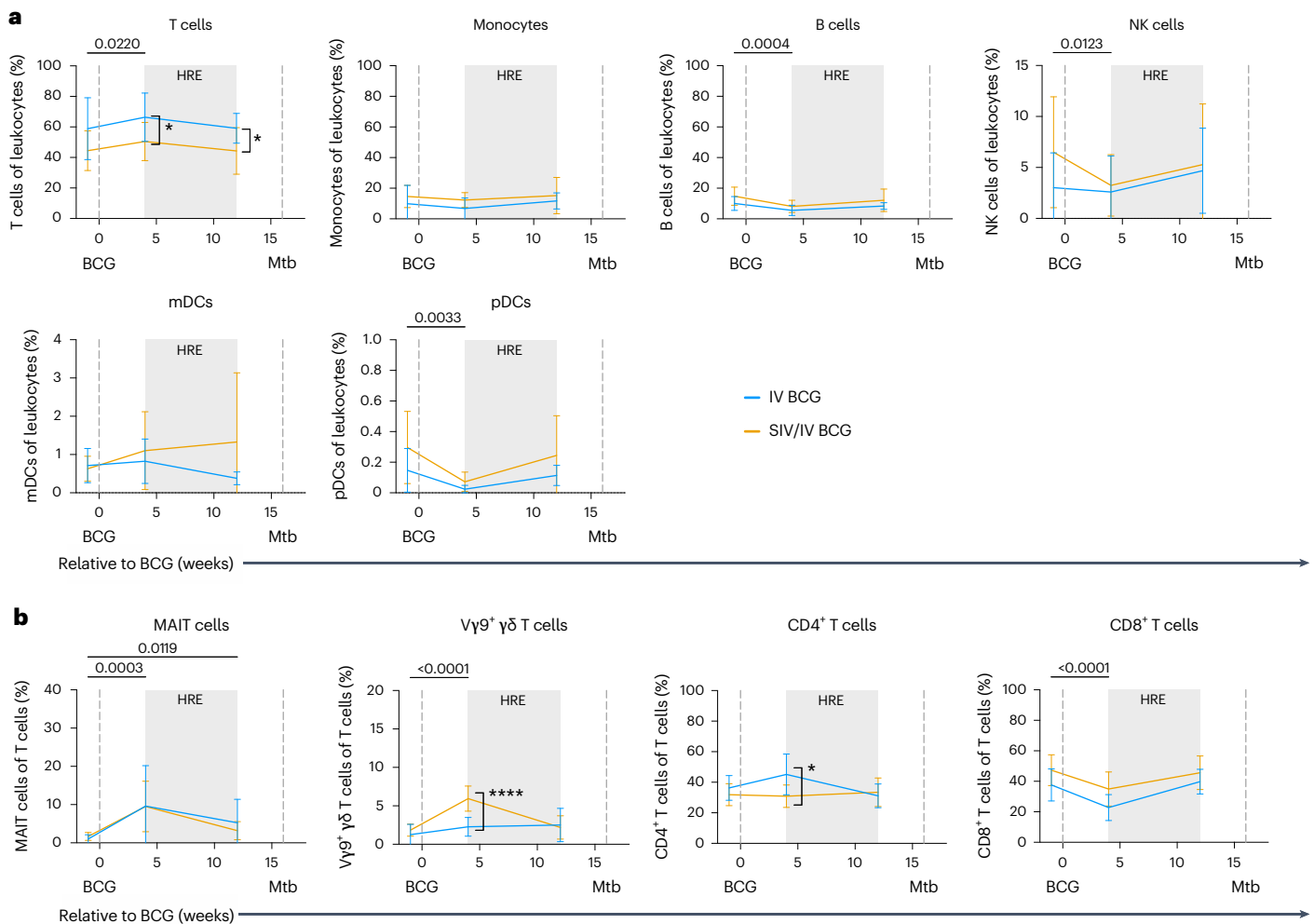
Fig. 3 | Frequencies of leukocyte and T cell subsets in PBMC after vaccination.
a, Frequencies of leukocyte subsets relative to BCG. mDCs, myeloid dendritic cells; pDCs, plasmacytoid dendritic cells. **b**, Frequencies of T cells and T cell subsets (MAIT, Vγ9^{+}, CD4^{+} and CD8^{+} T cells) relative to BCG. Data are mean and s.d. of SIV-naive (IV BCG, light blue) and SIV+ (SIV/IV BCG, gold) vaccinated animals. SIV-naive vaccinated animals: pre-BCG ($n = 7$), 4 weeks post-BCG ($n = 7$) and 12 weeks post-BCG ($n = 7$). SIV+ vaccinated animals: pre-BCG ($n = 12$), 4 weeks post-BCG ($n = 12$) and 12 weeks post-BCG ($n = 11$). Individual animal data are shown in Supplementary Data 6. Mixed effects models with subject as a random variable were used to assess mean differences among timepoints and vaccine groups. Timepoints were compared to 'pre-BCG' control using Dunnett's multiple comparison tests. Significant P values ($P < 0.05$) across time are shown above each graph. Significant differences determined by Mann–Whitney tests between vaccination groups at given timepoints are indicated by brackets and significant P values (not adjusted for multiple comparison) indicated: *$P < 0.05$ and ****$P < 0.0001$. Fixed effect test results, Dunnett's multiple comparisons and Mann–Whitney test results are reported in Supplementary Table 2b. All statistical tests were two-sided.

occurred between 4 and 8 weeks after Mtb co-infection in SIV+ animals[22]. We observed a similar effect here (Fig. 6b). IV BCG vaccination of SIV-naive MCM resulted in minimal granuloma formation and no apparent dissemination, recapitulating the results from our prior study in rhesus macaques[16] (Fig. 6b). Remarkably, most SIV+ vaccinated macaques also had minimal granuloma formation and dissemination, although two animals did show progressive disease by this metric (Fig. 6b). PET/CT imaging before necropsy revealed striking differences in TB disease between the unvaccinated and vaccinated animals (Fig. 6c). Both SIV-naive and SIV+ vaccinated animals had significantly less lung inflammation compared with their respective unvaccinated controls at necropsy, although 3 of the 12 SIV+ vaccinated animals did have increased lung FDG activity (Fig. 6d).

TB pathology was assessed at necropsy using an established scoring system[21]. IV BCG resulted in a significant reduction in lung pathology regardless of SIV, although there were two SIV+ vaccinated animals with high pathology scores (Fig. 6e). Multiple tissue samples were plated at time of necropsy and Mtb bacterial burden (the CFU)

was quantified. Tissues were isolated from all 7 SIV-naive vaccinated animals, and 9 out of 12 SIV+ vaccinated animals were completely sterile 12 weeks after Mtb challenge (Fig. 6f). As reported previously[22], SIV+ unvaccinated animals had significantly higher bacterial burden than SIV-naive unvaccinated animals, indicative of an immune defect due to SIV (Extended Data Fig. 4). IV BCG vaccination resulted in a significant reduction in pathology and Mtb burden across different tissue compartments (lung, thoracic lymph node and extrapulmonary sites), regardless of SIV status (Extended Data Fig. 5a–e). With protection from TB defined as a total thoracic Mtb burden <100 CFU[16], IV BCG conferred 100% protection in the SIV-naive animals (7 out of 7) and 75% protection in the SIV+ animals (9/12).

The three unprotected SIV+ vaccinated animals tended to have higher plasma viraemia levels (Extended Data Fig. 6a). Moreover, these three animals appeared to have elevated levels of circulating CD4^{+} T_FH cells and fewer CD4^{+} T cells in the airways during the IV BCG vaccination period (Extended Data Fig. 6b,c). These data suggest that at least two of the unprotected animals showed signs of progressive
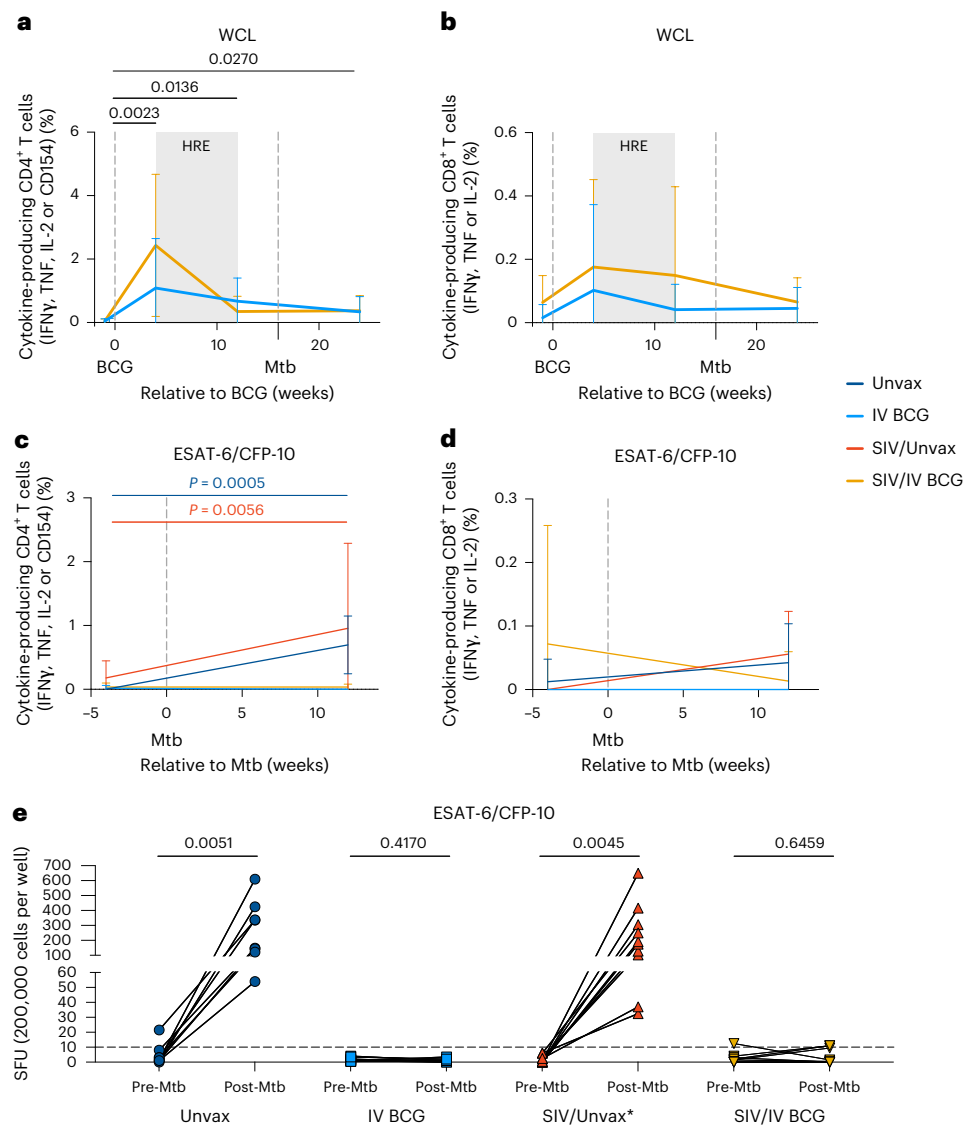
Fig. 4 | T cell response in PBMC after BCG vaccination and Mtb challenge.
a,b, Frequency of cytokine-responsive CD4$^+$ (**a**) and CD8$^+$ (**b**) T cells in PBMC after 14 h stimulation with H37Rv whole cell lysate relative to BCG vaccination. Mixed effects models with subject as a random variable were used to assess mean differences among timepoints and vaccine groups. Timepoints were compared with 'pre-BCG' control using Dunnett's multiple comparison tests. Significant P values ($P < 0.05$) across time are shown above each graph. Fixed effect test results and Dunnett's multiple comparisons are reported in Supplementary Table 2d. **c,d**, Frequency of cytokine-responsive CD4$^+$ (**c**) and CD8$^+$ (**d**) T cells in PBMC after 14 h stimulation with ESAT-6/CFP-10. Data shown in weeks relative to Mtb challenge. Linear mixed effects models were used to determine significant mean differences between time and animal group. Šidák's multiple comparisons test P values are reported in Supplementary Table 2d. Significant P values ($P < 0.05$) across time for each treatment group are shown above each graph. In **a–d**, data are mean and s.d. of Unvax (dark blue), IV BCG (light blue), SIV/Unvax (red) and

SIV/IV BCG (gold) animals. Unvaccinated animals (Unvax): pre-Mtb ($n = 8$) and 12 weeks post-Mtb ($n = 8$). SIV-naive vaccinated animals (IV BCG): pre-BCG ($n = 7$), 4 weeks post-BCG ($n = 7$), 12 weeks post-BCG/pre-Mtb ($n = 7$) and 12 weeks post-Mtb ($n = 7$). SIV+ unvaccinated (SIV/Unvax): pre-Mtb ($n = 4$) and 12 weeks post-Mtb ($n = 4$). SIV+ vaccinated animals (SIV/IV BCG): pre-BCG ($n = 12$), 4 weeks post-BCG ($n = 12$), 12 weeks post-BCG/pre-Mtb ($n = 11$) and 12 weeks post-Mtb ($n = 12$). Individual animal data are shown in Supplementary Data 7. **e**, IFNγ production in PBMC before and after Mtb challenge (12 weeks post-Mtb) by ELISpot. SFU, spot-forming units. Individual symbols and lines indicate individual animals. Unvax, pre-Mtb ($n = 8$) and post-Mtb ($n = 8$); IV BCG, pre-BCG ($n = 7$) and post-Mtb ($n = 7$); SIV/Unvax with historical controls, pre-Mtb ($n = 8$) and post-Mtb ($n = 8$); SIV/IV BCG, pre-BCG ($n = 10$) and post-Mtb ($n = 9$). Paired t-tests were used to determine significance within each group. P values are shown. All statistical tests were two-sided.

SIV infection. Progressive SIV impairs immunity, especially through the depletion of CD4$^+$ T cells[30,42]. The high viral replication in these animals may have compromised the ability of IV BCG to elicit a successful anti-mycobacterial response, resulting in poor protection against Mtb.

Overall, these data demonstrate that IV BCG vaccination resulted in complete protection against Mtb in SIV-naive animals. Furthermore, we show that high-order protection against Mtb is achievable in SIV+ animals.

Discussion

Protection against TB in SIV+ macaques has not been previously demonstrated. Here we show that IV BCG can confer sterilizing immunity in 75% of SIV+ macaques. In addition, we recapitulated our previously published robust protection and sterilizing immunity provided by IV BCG in SIV-naive rhesus macaques[16] in 100% of MCM, a different SIV-naive macaque species. Immune responses to IV BCG were similar in SIV-naive and SIV+ macaques, with a robust and sustained expansion of mycobacterial-specific CD4$^+$ and CD8$^+$ T cells in the airways, lower
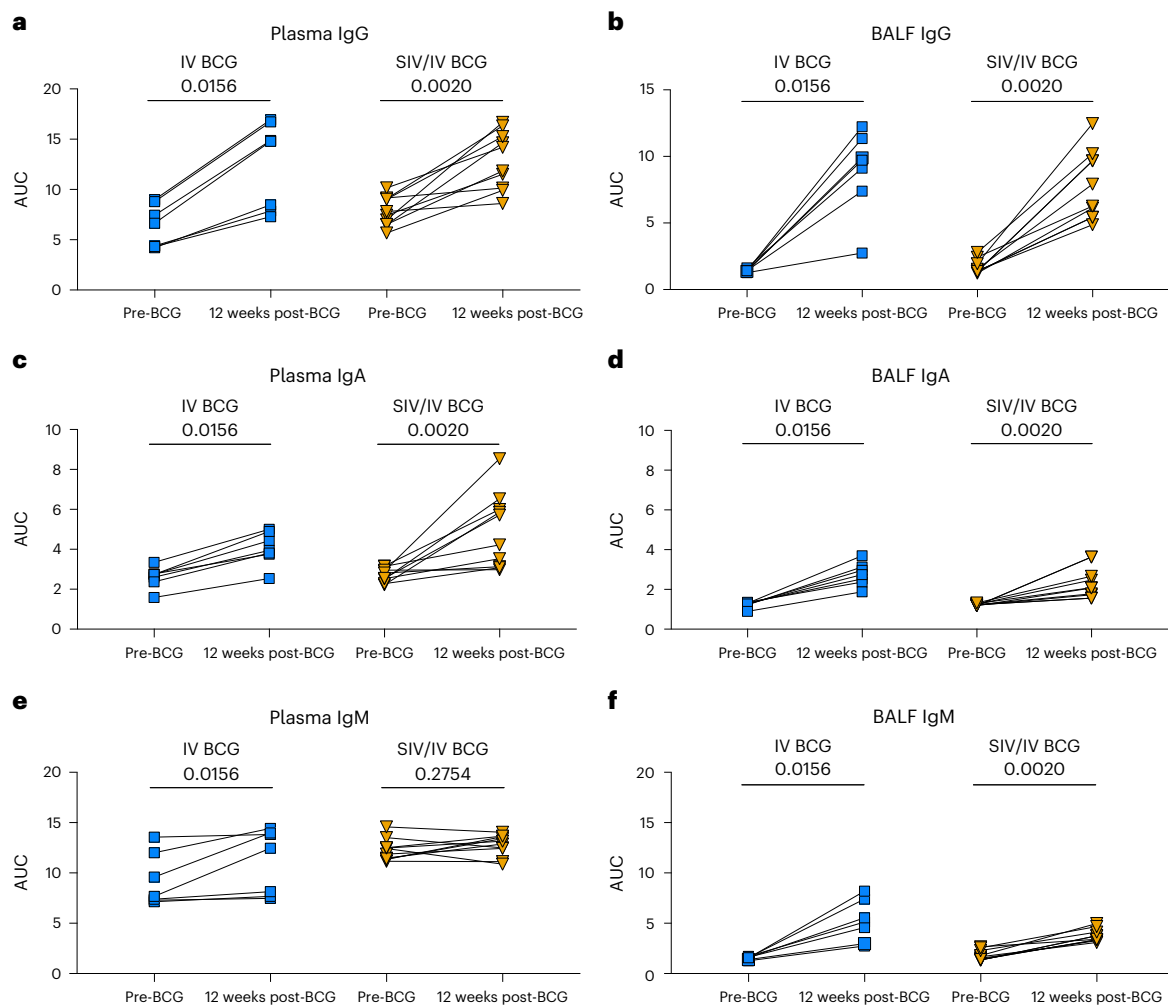
Fig. 5 | Mycobacterial-specific antibodies in plasma and BALF following BCG vaccination. a–f, Antibodies specific for H37Rv whole cell lysate were assessed by ELISA for both vaccinated groups: plasma IgG (**a**), BALF IgG (**b**), plasma IgA (**c**), BALF IgA (**d**), plasma IgM (**e**) and BALF IgM (**f**). AUC was determined by calculating the area under the dilution series curve using GraphPad Prism. Individual animals indicated by symbols for IV BCG (light-blue square; $n = 7$) and SIV/IV BCG (gold, down-pointing triangle; $n = 12$). Wilcoxon paired signed rank tests were performed to determine significance. P values are shown.

but significant increases in γδ T cells and MAIT cells, and enhanced mycobacterial-reactive antibody responses in blood and airways.

HIV/SIV infection is known to impair immune responses in their respective hosts. One concern of HIV/SIV infection is whether infection will interfere with vaccine-elicited immune responses in PLWHIV and NHP[43,44]. Collectively, our data indicate that SIV infection did not drastically impair the generation of mycobacterial-specific T cell or antibody responses in airways and blood. We previously reported an influx of mycobacterial-specific CD4+ and CD8+ T cells in the airways of IV BCG-vaccinated SIV-naive rhesus macaques, which correlated with protection[16,45]. Here, we observed a similar influx of airway CD4+ and CD8+ T cells, and increased circulating CD4+ T cell frequencies, in SIV+ and SIV-naive animals shortly after IV BCG vaccination. Polyfunctional T_H17 T cells in airways following mucosal BCG vaccination have been correlated with protection[15] and are associated with better Mtb control in granulomas[46]. We observed here an influx of IL-17A-producing CD4+ T cells in airways and an increase in circulating T_H1/T_H17 (T_H1^*) CD4+ T cell frequencies in both SIV+ and SIV-naive groups after IV BCG vaccination. Mycobacterial-specific antibodies, which have been associated with IV BCG efficacy and Mtb control[20,47], increased in plasma and airways following IV BCG vaccination, regardless of SIV status.

It is important to note that the vaccinated animals were treated with anti-mycobacterial drugs beginning within 4 weeks of vaccination as an added precaution against disseminated BCG in SIV+ animals. Yet the IV BCG-induced immune responses and protection were not diminished but rather maintained in all SIV-naive macaques and most SIV+ macaques. These data suggest that BCG can be killed soon after vaccination without loss of protection. IV BCG has been shown to induce an influx of CD3+ T cells in lung tissue and airways and CD11c+ antigen-presenting cells in lung tissue 1 month after vaccination in SIV-naive rhesus macaques[16]. This early influx of cells to airways and lung, around the same time frame we initiated HRE, may indicate that sterilizing immune mechanisms are established within the first month after vaccination, although exact BCG kill kinetics were not measured in our study and it is possible that longer antigen exposure is required for durable protection.

We noted a transient spike in plasma viraemia 2 weeks after IV BCG vaccination, which was mirrored by an increased frequency of circulating CCR5+ CD4+ T cells 2 weeks later. BCG vaccination has been shown to increase these cells in both HIV-exposed infants and infant macaques[48,49]. Given that CCR5+ CD4+ T cells are a target of SIV[32], the observed spike in viraemia is probably due to the expansion of infectable cells induced by BCG. This transient burst of SIV replication following IV BCG may increase the viral reservoirs in tissues and represent a safety signal for TB vaccines in the context of HIV infection. However, this effect may be mitigated by concurrent ART.
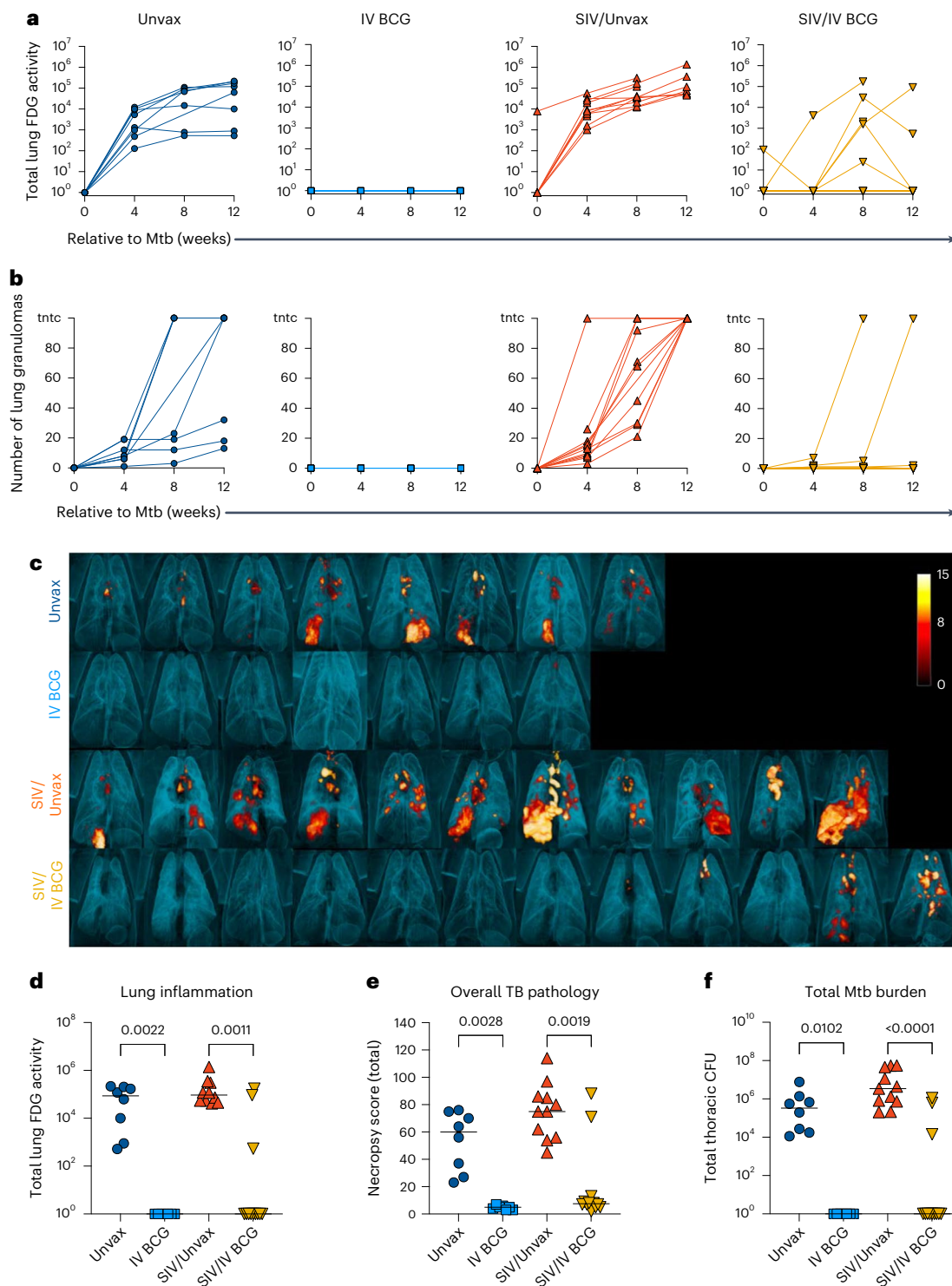
Fig. 6 | Protection against Mtb challenge in BCG-vaccinated groups. a, Total FDG activity (lung inflammation) relative to Mtb challenge, measured by PET/CT imaging. Lines indicate individual animals. **b**, Number of lung granulomas relative to Mtb challenge. Animals with granuloma numbers >100 are indicated as too numerous to count (tntc). At 4 and 8 weeks, granulomas were counted by CT, whereas at 12 weeks, granulomas were counted by gross pathology. **c**, Three-dimensional renderings of PET/CT images of individual animals taken at necropsy. **d–f**, Lung inflammation (**d**), overall TB pathology (**e**) and total Mtb burden (thoracic CFU) (**f**) at necropsy. Each point indicates an individual animal and horizontal bars indicate group medians (Unvax, $n = 8$; IV BCG, $n = 7$; SIV/Unvax, $n = 11$; SIV/IV BCG, $n = 12$). Kruskal–Wallis tests were performed with Dunn's multiple comparisons between SIV-naive, vaccinated and unvaccinated groups (dark-blue circles and light-blue squares, respectively), and SIV+, vaccinated and unvaccinated groups (red, up-pointing triangle and gold, down-pointing triangle, respectively). P values are shown. All statistical tests were two-sided.

Three SIV+ vaccinated animals were unprotected from Mtb challenge. These animals tended to have a higher viral setpoint, more circulating T_{FH} and fewer CD4+ T cells in BAL, suggesting that unprotected animals had progressive SIV infections[30,50,51]. In a study of BCG co-infection of SIV+ rhesus macaques, animals with high plasma viraemia (>10^6 copies ml^-1) exhibited fewer circulating CD4+ T cells and disseminated BCG[52]. Airways were not sampled in that study. While we did not observe disseminated BCG in the three unprotected animals, it is possible that the progressive SIV infection ablated the development of an effective anti-mycobacterial T cell response elicited by IV BCG. Conversely, the SIV+ animals that were protected by IV BCG tended to have more CD4+ T cells in the airways and better-controlled SIV.

There are several limitations to this study. SIV infection in MCM was quasi-pathogenic: some SIV+ vaccinated animals were able to naturally control SIV replication, while others (n = 2) maintained high plasma viraemia (>10^6 copies ml^-1). While we do believe there is some level of immune defect given that, as shown previously[22] as well as here, unvaccinated SIV+ MCM co-infected with Mtb have a higher bacterial burden regardless of viraemic control compared with animals infected with Mtb alone, we recognize that animals with better-controlled SIV plasma viraemia were completely protected. This may highlight the need for viraemic control, achieved either naturally or by ART, to ensure IV BCG-elicited sterilizing immunity in SIV+ animals. The link between sterilizing immunity and viraemic control will be explored in future studies. The 4-month vaccination period, chosen to minimize possible confounding variables introduced by SIV pathogenesis (for example, lymphoma, thrombocytopaenia and so on), did not assess vaccine durability and sterilizing immunity, which may be due to, in part, short-lived changes in innate immune cells. BCG has been shown to enhance innate immunity against TB through elevated cytokine production of monocytes and epigenetic modifications of haematopoietic stem cells, referred to as trained immunity[53–56]. The effect of BCG on trained immunity has been demonstrated to last 3 months to 1 year after IV vaccination in healthy volunteers[57,58]. While previous data suggest that trained immunity may not occur with IV BCG in SIV-naive rhesus macaques (that is, no culturable BCG from the bone marrow and no increase in innate activation to non-specific stimuli)[16], this aspect of immunity was not investigated in the current study. It is possible that protection may wane due to the loss of innate immune cell functions over time.

There are still many unknowns about sterilizing immunity generated by IV BCG in SIV+ macaques. First, it is not yet known precisely how long BCG needs to be alive to elicit protection. We do not know the exact kill kinetics of HRE in our system and, therefore, the timing of when BCG is fully cleared. A self-limiting auxotrophic BCG strain may represent an effective alternative without the need for a post-vaccination antibiotic regimen[59]. Second, the durability of IV BCG-elicited protection is unknown, especially in an immunocompromised host. Studies with longer vaccine intervals are needed to determine durability of protection and immune correlates associated with long-lived immunity. Third, alternative routes of administration, such as mucosally delivered BCG[15,60] or MTBVAC[54,61], have yet to be explored in SIV-infected animals. Overall, this study shows robust vaccine-elicited protection against Mtb infection and disease using a NHP model of HIV. Furthermore, this study establishes a model to identify correlates of protection in the context of pre-existing SIV/HIV and lays the groundwork for future studies to develop effective TB vaccine regimens for PLWHIV.

Methods

Animals

Adult Mauritian cynomolgus macaques (*Macaca fascicularis*; age >4 years old; n = 40) were obtained from Bioculture US (Extended Data Table 1). MHC haplotype was determined by MiSeq sequencing and animals with the presence of at least one copy of the M1 MHC haplotype were selected for this study[62,63].

Animal protocols and procedures were approved by the University of Pittsburgh Institutional Animal Care and Use Committee, which adheres to guidelines established in the Animal Welfare Act and the Guide for the Care and Use of Laboratory Animals, as well as the Weatherall Report (8th Edition). The University is fully accredited by the Association for Assessment and Accreditation of Laboratory Animal Care International (accreditation number 000496), and its Office of Laboratory Animal Welfare assurance number is D16-00118. The Institutional Animal Care and Use Committee reviewed and approved the study protocols 15035407 and 18032418, under assurance numbers A3187-01 and D16-00118, respectively.

Animal welfare was monitored twice daily for overall physical health (weight, appetite, activity level, and so on) as described previously[23]. Animals were monitored closely following Mtb challenge for clinical signs of TB (for example, weight loss, tachypnoea, dyspnoea or coughing). In addition, regular PET/CT imaging was conducted to monitor TB progression. Animals were sedated for all veterinary procedures (for example, blood draws) using ketamine or other approved drugs. Veterinary technicians monitored animals especially closely for any signs of pain or distress and provided appropriate supportive care (for example, dietary supplementation and rehydration) and treatments (analgesics) when necessary. Any animal considered to have advanced disease or intractable pain from any cause, was deemed to have reached the humane endpoint, sedated with ketamine and humanely euthanized using sodium pentobarbital.

SIV infection

Vaccinated and unvaccinated macaques designated for SIV infection were infected intrarectally with SIVmac239 (3,000 50% tissue culture infectious dose IU). Plasma viraemia was monitored serially by quantitative PCR (qPCR) as previous described[64,65]. Viral RNA was isolated using the Maxwell Viral Total Nucleic Acid Purification Kit (Promega) and reversed transcribed using the TaqMan Fast Virus 1-Step quantitative reverse transcription PCR (qRT–PCR) Kit (Invitrogen). DNA was quantified on a LightCycler 480 (Roche).

BCG vaccination

BCG Danish Strain 1331 (Statens Serum Institute) was expanded (by Aeras, now AVI) and frozen at approximately, 3×10^8 CFU ml^-1. Just before BCG injection, BCG was thawed and diluted in sterile PBS to approximately 5×10^7 CFU ml^-1 (actual: 8×10^7 CFU ml^-1). IV BCG was injected into the left saphenous vein in a volume of 1 ml. An aliquot of inoculum was plated on 7H11 agar and CFU was enumerated 3 weeks later to ensure an accurate input inoculum.

HRE administration

Isoniazid (Teva Pharmaceuticals; 15 mg kg^-1, per os), rifampin (Darmerica; 20 mg kg^-1, per os) and ethambutol (Lupin Pharmaceuticals; 55 mg kg^-1, p.o.), referred to together as HRE, obtained from The Pet Apothecary, was administered once daily for 8 weeks starting 3–4 weeks after IV BCG vaccination. Unvaccinated animals received HRE to minimize any confounding effects due to antibiotic therapy.

Mtb challenge

All animals were infected with a low dose (4–21 CFU) of Mtb Erdman via bronchoscopic instillation, as described previously[21].

Clinical and microbiological monitoring

All animals were assessed twice daily for general health over the entirety of the study. Blood cultures were performed 2 weeks after IV BCG to assess BCG CFU ml^-1. Blood was plated on two 7H11 plates at 500 μl per plate, incubated for 21 days and colonies were enumerated. Following Mtb challenge, animals were monitored closely for clinical signs of TB (coughing, weight loss, tachypnoea, dyspnoea and so on) following Mtb challenge. Monthly gastric aspirates and bronchoalveolar lavage

samples were tested for Mtb growth. Blood was drawn at regular intervals to measure erythrocyte sedimentation rate and to provide PBMC and plasma.

PBMC and BAL processing

PBMC were isolated from blood using Ficoll-Paque PLUS gradient separation (GE Healthcare Biosciences). Single-cell suspensions were cryopreserved in foetal bovine serum containing 10% dimethylsulfoxide in liquid nitrogen. BAL wash fluid (4 × 10 ml washes of PBS) was pelleted and an aliquot of wash fluid (15 ml) was cryopreserved. The remaining cells were resuspended into ELISpot medium (Roswell Park Memorial Institute medium 1640, 10% heat-inactivated human albumin, 1% L-glutamine and 1% 4-(2-hydroxyethyl)-1-piperazineethanesulfonic acid) and counted. BAL cells were then divided into their appropriate flow cytometry assay depending on cell yield.

Multiparameter flow cytometry

Longitudinal BAL and PBMC samples were stained for leukocyte composition (phenotype) or antigen-specific T cell responses. In general, BAL cells were stained immediately and PBMC were cryopreserved and batch-analysed at the end of the study.

For BAL analyses, cells were counted and aliquoted into a 96-well plate for either phenotype or intracellular cytokine responses (1 × 10^6 cells per well). In cases where total BAL cell counts were low, cells were prioritized for the 14-h stimulation assay. For the phenotype panel, cells were reconstituted in 500 nM dasatinib in ELISpot media to improve MHC class I-related protein (MR1) (5-OP-RU; BV421) tetramer staining. Cells were incubated with MR1 tetramer (National Institute of Health (NIH) Tetramer Core Facility) for 30 min at 4 °C. The MR1 technology was developed jointly by J. McCluskey, J. Rossjohn and D. Fairlie, and the material was produced by the NIH Tetramer Core Facility as permitted to be distributed by the University of Melbourne. Cells were then washed and stained for viability (Zombie Live/Dead near IR; Invitrogen) for 10 min at room temperature (25 °C). Cells were then washed, incubated with surface antibody cocktail for 20 min at 4 °C, and fixed with 1% paraformaldehyde for 15 min. For the intracellular cytokine assay, cells were aliquoted (1 × 10^6 cells per well) into either a media control well, PPD well (20 μg ml^−1; AJ Vaccines) or ESAT-6/CFP-10 overlapping peptide pools (1 μg ml^−1 each; BEI Resources). Stimulators were added and incubated for 2 h, then brefeldin A (1 μg ml^−1; BioLegend, cat. no. 420601) and monensin (1 μg ml^−1; BioLegend, cat. no. 420701) was added for the remainder of the stimulation time (12 h). Cells were washed and surface markers were stained similarly as described for the phenotype panel. However, after paraformaldehyde fixation, cells were permeabilized with BD Cytofix/Cytoperm (BD, cat. no. 554714) for 10 min at room temperature. Intracellular markers were stained for 20 min at room temperature. Stained BAL cells were run within 2 days of staining.

Flow cytometry of BAL was performed using a Cytek Aurora (BD, SpectroFlo v2.2). Flow cytometry standard files were analysed using FlowJo software for Macintosh (version 10.1). Frequencies relative to live leukocytes were used to calculate cell counts per BAL collection (Fig. 2). In brief, cell counts enumerated on a haemocytometer were multiplied by the frequency of the cell population of interest (for example, T cells) relative to live leukocytes. BAL samples with low viability (<70%) or elevated background autofluorescence were excluded from analyses. Lastly, due to the coronavirus disease 2019 pandemic, several BAL collections were not collected to ensure the health and safety of our technical staff. Therefore, the number of BAL samples indicated in Fig. 2 are reflective of samples collected before and over the course of the coronavirus disease 2019 pandemic and met the inclusion criteria described above. Individual animal data are shown in Supplementary Data 1.

For PBMC analyses, cells were divided to be stained for phenotype or 14-h stimulation as previously described[16]. PBMC stimulators include: H37Rv whole cell lysate (20 μg ml^−1; BEI Resources) and ESAT-6/CFP-10 peptide pools (1 μg ml^−1 each). Cells were stained as follows: cells were stained with MR1 tetramer for 20 min, washed twice with PBS/bovine serum albumin (BSA) (0.1%), then stained with viability dye for 20 min, washed twice with PBS/BSA (0.1%) and incubated with human fragment crystallizable receptor blocking reagent (Miltenyi); surface markers were stained for 20 min and washed three times with PBS/BSA (0.1%); cells were permeabilized with BD Cytofix/Cytoperm (BD, cat. no. 554714) for 20 min; and intracellular markers were stained for 30 min. Data were acquired on a modified BD LSR Fortessa (FACS Diva v9.3) and analysed in FlowJo software for Macintosh (version 10.8.1). Gating strategies are shown in Supplementary Data 1–4. All cytokine data presented are background-subtracted. Antibodies used in BAL and PBMC panels are listed in Supplementary Table 1.

ELISPOT

ELISPOT was performed as previously described[16]. In brief, 96-well plates were coated with monkey IFNγ antibody (clone MT126L, 15 μg ml^−1), incubated overnight at 4 °C and wells were washed with sterile PBS. Wells were then blocked for 2 h at 37 °C at 5% CO_2 with ELISpot medium (Roswell Park Memorial Institute medium 1640 + 10% human albumin + 1% L-glutamine + 1% 4-(2-hydroxyethyl)-1-piperazineethanesulfonic acid) and washed with sterile PBS. Frozen PBMC were thawed and enumerated by haemocytometer. Cells were aliquoted into wells at 2 × 10^5 cells per well (150 μl). Stimulators or ELISPOT media control (50 μl) were added to the appropriate wells, and plates were incubated at 37 °C at 5% CO_2 for 40–48 h. The stimulators and the final concentrations used in this assay include: CFP peptide pools (2 μg ml^−1), ESAT-6 peptide pools (2 μg ml^−1), CFP-10 peptide pools (2 μg ml^−1) and phorbol 12,13-dibutyrate and ionomycin (12.5 μg ml^−1 and 37.5 μg ml^−1, respectively). Wells were washed with PBS and incubated with biotinylated anti-human IFNγ antibody (clone 7-B6, 2.5 μg ml^−1) for 2 h at 37 °C at 5% CO_2. Wells were again washed with PBS and incubated this time with streptavidin-linked horseradish peroxidase (1:100 dilution in PBS + 0.5% foetal bovine serum) for 45 min at 37 °C at 5% CO_2. After washing with PBS for a third time, 3-amino-9-ethylcarbazole substrate was added to the wells and the plate was developed for 5–8 min in the dark (3-amino-9-ethylcarbazole kit). Finally, wells were washed with diH_2O, fixed with 2% PFA for 10 min, washed with PBS and dried overnight. Spot forming units were counted manually on an ELISpot reader (ImmunoSpot v5.1).

Serology

The antibody ELISAs were performed as previously described by Darrah et al. 2020 (ref. 16). MaxiSorp ELISA plates (96 wells; Thermo Scientific) were coated with 100 μl of H37Rv WCL at a concentration of 1 μg ml^−1 per well at 4 °C overnight. The coated plates were blocked with 100 μl of 1× blocking solution (PBS + 10% FBS) for 2 h at room temperature. Plates were washed six times with PBS-Tween between each step. Plasma or 10× BAL concentrate from each animal were 1:5 serially diluted. A volume of 100 μl was added and incubated at 37 °C for 2 h. After 2 h, plates were incubated with 100 μl of diluted horseradish peroxidase-conjugated antibody. Plates were incubated for 1 h at room temperature. A final wash step was done, samples were incubated for approximately 12 min with 100 μl Ultra TMB ELISA substrate (Invitrogen, cat. no. 34029). The reaction was stopped by adding 100 μl of 2N sulfuric acid. The plates were read with a Promega Glomax Multi detection system (v1.3.2) at 450 nm. Analysis was done using GraphPad Prism software (version 8.2.1). Data are presented as area under the curve (AUC).

PET/CT

Radiolabeled 2-deoxy-2-(^18F)fluoro-D-glucose (FDG) PET/CT imaging was performed 4, 8 and 12 weeks after Mtb challenge. Imaging was performed using a MultiScan LFER-150 PET/CT scanner (Mediso Medical

Imaging Systems) housed within our biosafety level 3 facility as previously described[66,67]. Co-registered PET/CT images were analysed using OsiriX MD software (version 12.5.2, Pixmeo) to enumerate granulomas and to calculate the total FDG avidity of the lungs, exclusive of lymph nodes, which are a quantitative measure of total inflammation in the lungs[66,68]. For historical controls, PET/CT scans were performed using a microPET Focus 220 preclinical PET scanner (Siemens Molecular Solutions) and a clinical eight-slice helical CT scanner (NeuroLogica Corporation)[68]. Thoracic lymphadenopathy and extrapulmonary dissemination of Mtb to the spleen and/or liver were also assessed qualitatively on these scans.

Necropsy, pathology and bacterial load
Necropsies were performed at around 12 weeks following Mtb challenge as previously described[22,23] We used an established scoring system to quantitatively assess gross pathology[21]. Pathology scores were calculated and reflect overall TB disease burden for each animal. Tissue samples were divided and a portion were fixed in 10% neutral-buffered formalin for histopathology; the remainder were homogenized to a single-cell suspension as described previously[21]. Serial dilutions of these homogenates were plated onto 7H11 agar and incubated at 37 °C at 5% CO_2 for 3 weeks, and colonies were enumerated. Bacterial burden in lungs, thoracic lymph nodes, liver and spleen, as well as total thoracic CFU, were calculated as described previously[21]. Neutral-buffered formalin-fixed tissue was embedded in paraffin, sectioned and stained with haematoxylin and eosin for histopathologic examination.

Statistics including power analysis
We used total thoracic bacterial burden (log_{10}) as the primary outcome variable with a pooled standard deviation (s.d.) of 1.09 (calculated by averaging s.d. of all groups) for a two-sided test and adjusted the type I error for two comparisons ($\alpha = 0.025$). For the unvaccinated ($n = 8$) and IV BCG ($n = 7$) comparison, we obtained 83.0% power to detect a mean difference of 2 in bacterial burden. For the SIV/Unvaccinated ($n = 11$) and SIV/IV BCG ($n = 12$) comparison, we obtained 97.0% power to detect a mean difference of 2. Normality was tested by using Shapiro–Wilk test. Significance of plasma viraemia relative to BCG within SIV+ groups was assessed using repeated measure one-way analyses of variance (ANOVAs) paired with Dunnett's multiple comparisons tests to assess significance relative to 'pre-BCG'. For all other longitudinal comparisons between vaccinated groups, linear mixed effects models with subject as a random variable were used (Supplementary Table 2). Fixed effect tests were used to assess differences among timepoints and vaccine groups (including an interaction term of time × vaccine). Timepoints were compared with 'pre-BCG' control using Dunnett's multiple comparison tests. When a treatment effect was present (that is, SIV infection), we performed Mann–Whitney tests at individual timepoints (not adjusting for multiple comparisons). For comparisons among all four groups across specific timepoints (for example, pre- versus post-Mtb), linear mixed effects models with Šidák's multiple comparisons were used (Supplementary Table 2). Comparisons between pre and post (relative to either BCG or Mtb challenge) were tested using either paired *t*-tests or Wilcoxon paired signed rank tests, depending on normality. Kruskal–Wallis tests were performed with Dunn's multiple comparisons between SIV-naive, vaccinated and unvaccinated groups, and SIV+, vaccinated and unvaccinated groups, for necropsy outcome data (for example, lung inflammation, TB pathology and Mtb burden). Statistical tests were performed in Prism (version 8.2.1; GraphPad). All tests were two-sided and statistical significance was designated at a *P* value of <0.05.

Reporting summary
Further information on research design is available in the Nature Portfolio Reporting Summary linked to this article.

Data availability
All relevant data are available from the corresponding author upon reasonable request. Source data are provided with this paper.

References
1. *Global Tuberculosis Report 2022* (World Health Organization, 2022).
2. Houben, R. M. et al. Human immunodeficiency virus associated tuberculosis more often due to recent infection than reactivation of latent infection. *Int J. Tuberc. Lung Dis.* **15**, 24–31 (2011).
3. Waters, R. et al. The Mtb–HIV syndemic interaction: why treating *M. tuberculosis* infection may be crucial for HIV-1 eradication. *Future Virol.* **15**, 101–125 (2020).
4. Miner, M. D. et al. Developing tuberculosis vaccines for people with HIV: consensus statements from an international expert panel. *Lancet HIV* **9**, e791–e800 (2022).
5. Mangtani, P. et al. Protection by BCG vaccine against tuberculosis: a systematic review of randomized controlled trials. *Clin. Infect. Dis.* **58**, 470–480 (2014).
6. Fine, P. E. M., Carneiro, I. A. M., Milstein, J. B. & Clements, J. C. *Issues Relating to the Use of BCG in Immunization Programmes: A Discussion Document* (World Health Organizaiton, 1999).
7. *Weekly Epidemiological Record* Vol. 8, 73–96 (World Health Organization, 2018).
8. Darrah, P. A. et al. Boosting BCG with proteins or rAd5 does not enhance protection against tuberculosis in rhesus macaques. *NPJ Vaccines* **4**, 21 (2019).
9. Vierboom, M. P. M. et al. Evaluation of heterologous prime-boost vaccination strategies using chimpanzee adenovirus and modified vaccinia virus for TB subunit vaccination in rhesus macaques. *NPJ Vaccines* **5**, 39 (2020).
10. Woodworth, J. S. et al. A *Mycobacterium tuberculosis*-specific subunit vaccine that provides synergistic immunity upon co-administration with Bacillus Calmette–Guérin. *Nat. Commun.* **12**, 6658 (2021).
11. Nieuwenhuizen, N. E. & Kaufmann, S. H. E. Next-generation vaccines based on bacille Calmette–Guérin. *Front. Immunol.* **9**, 121 (2018).
12. Nemeth, J. et al. Contained *Mycobacterium tuberculosis* infection induces concomitant and heterologous protection. *PLoS Pathog.* **16**, e1008655 (2020).
13. Cadena, A. M. et al. Concurrent infection with *Mycobacterium tuberculosis* confers robust protection against secondary infection in macaques. *PLoS Pathog.* **14**, e1007305 (2018).
14. Hansen, S. G. et al. Prevention of tuberculosis in rhesus macaques by a cytomegalovirus-based vaccine. *Nat. Med.* **24**, 130–143 (2018).
15. Dijkman, K. et al. Prevention of tuberculosis infection and disease by local BCG in repeatedly exposed rhesus macaques. *Nat. Med.* **25**, 255–262 (2019).
16. Darrah, P. A. et al. Prevention of tuberculosis in macaques after intravenous BCG immunization. *Nature* **577**, 95–102 (2020).
17. Sharpe, S. et al. Alternative BCG delivery strategies improve protection against *Mycobacterium tuberculosis* in non-human primates: protection associated with mycobacterial antigen-specific CD4 effector memory T-cell populations. *Tuberculosis* **101**, 174–190 (2016).
18. Barclay, W. R., Anacker, R. L., Brehmer, W., Leif, W. & Ribi, E. Aerosol-induced tuberculosis in subhuman primates and the course of the disease after intravenous BCG vaccination. *Infect. Immun.* **2**, 574–582 (1970).
19. Anacker, R. L. et al. Superiority of intravenously administered BCG and BCG cell walls in protecting rhesus monkeys (*Macaca mulatta*) against airborne tuberculosis. *Z. Immunitatsforsch. Exp. Klin. Immunol.* **143**, 363–376 (1972).

20. Irvine, E. B. et al. Robust IgM responses following intravenous vaccination with bacille Calmette–Guérin associate with prevention of *Mycobacterium tuberculosis* infection in macaques. *Nat. Immunol.* **22**, 1515–1523 (2021).

21. Maiello, P. et al. Rhesus macaques are more susceptible to progressive tuberculosis than cynomolgus macaques: a quantitative comparison. *Infect. Immun.* **86**, e00505–17 (2018).

22. Rodgers, M. A. et al. Preexisting simian immunodeficiency virus infection increases susceptibility to tuberculosis in mauritian cynomolgus macaques. *Infect. Immun.* **86**, e00505–e00517 (2018).

23. Larson, E. C. et al. Pre-existing simian immunodeficiency virus infection increases expression of T cell markers associated with activation during early *Mycobacterium tuberculosis* coinfection and impairs TNF responses in granulomas. *J. Immunol.* **207**, 175–188 (2021).

24. Wiseman, R. W. et al. Haplessly hoping: macaque major histocompatibility complex made easy. *ILAR J.* **54**, 196–210 (2013).

25. Budde, M. L. et al. Specific CD8+ T cell responses correlate with control of simian immunodeficiency virus replication in Mauritian cynomolgus macaques. *J. Virol.* **86**, 7596–7604 (2012).

26. Green, A. M., Difazio, R. & Flynn, J. L. IFN-γ from CD4 T cells is essential for host survival and enhances CD8 T cell function during *Mycobacterium tuberculosis* infection. *J. Immunol.* **190**, 270–277 (2013).

27. Allie, N. et al. Prominent role for T cell-derived tumour necrosis factor for sustained control of *Mycobacterium tuberculosis* infection. *Sci. Rep.* **3**, 1809 (2013).

28. Pollock, K. M. et al. T-cell immunophenotyping distinguishes active from latent tuberculosis. *J. Infect. Dis.* **208**, 952–968 (2013).

29. Song, X., He, X., Li, X. & Qian, Y. The roles and functional mechanisms of interleukin-17 family cytokines in mucosal immunity. *Cell Mol. Immunol.* **13**, 418–431 (2016).

30. Okoye, A. A. & Picker, L. J. CD4(+) T-cell depletion in HIV infection: mechanisms of immunological failure. *Immunol. Rev.* **254**, 54–64 (2013).

31. Lederman, M. M., Penn-Nicholson, A., Cho, M. & Mosier, D. Biology of CCR5 and its role in HIV infection and treatment. *JAMA* **296**, 815–826 (2006).

32. Jasinska, A. J., Pandrea, I. & Apetrei, C. CCR5 as a coreceptor for human immunodeficiency virus and simian immunodeficiency viruses: a prototypic love–hate affair. *Front. Immunol.* **13**, 835994 (2022).

33. Becattini, S. et al. T cell immunity. Functional heterogeneity of human memory CD4+ T cell clones primed by pathogens or vaccines. *Science* **347**, 400–406 (2015).

34. Nikitina, I. Y. et al. Th1, Th17, and Th1Th17 lymphocytes during tuberculosis: Th1 lymphocytes predominate and appear as low-differentiated CXCR3+CCR6+ cells in the blood and highly differentiated CXCR3+/−CCR6− cells in the lungs. *J. Immunol.* **200**, 2090–2103 (2018).

35. Chattopadhyay, P. K., Yu, J. & Roederer, M. Live-cell assay to detect antigen-specific CD4+ T-cell responses by CD154 expression. *Nat. Protoc.* **1**, 1–6 (2006).

36. Coppola, M. et al. Differences in IgG responses against infection phase related *Mycobacterium tuberculosis* (Mtb) specific antigens in individuals exposed or not to Mtb correlate with control of TB infection and progression. *Tuberculosis* **106**, 25–32 (2017).

37. Fischinger, S. et al. A *Mycobacterium tuberculosis* specific IgG3 signature of recurrent tuberculosis. *Front. Immunol.* **12**, 729186 (2021).

38. Nziza, N. et al. Defining discriminatory antibody fingerprints in active and latent tuberculosis. *Front. Immunol.* **13**, 856906 (2022).

39. Woods, C. R. False-positive results for immunoglobulin M serologic results: explanations and examples. *J. Pediatr. Infect. Dis. Soc.* **2**, 87–90 (2013).

40. Gehin, J. E. et al. Rheumatoid factor and falsely elevated results in commercial immunoassays: data from an early arthritis cohort. *Rheumatol. Int* **41**, 1657–1665 (2021).

41. Oka, S. et al. False-positive detection of IgM anti-severe acute respiratory syndrome coronavirus 2 antibodies in patients with rheumatoid arthritis: possible effects of IgM or IgG rheumatoid factors on immunochromatographic assay results. *SAGE Open Med.* **10**, 20503121221088090 (2022).

42. Corleis, B. et al. HIV-1 and SIV infection are associated with early loss of lung interstitial CD4+ T cells and dissemination of pulmonary tuberculosis. *Cell Rep.* **26**, 1409–1418.e1405 (2019).

43. El Chaer, F. & El Sahly, H. M. Vaccination in the adult patient infected with HIV: a review of vaccine efficacy and immunogenicity. *Am. J. Med.* **132**, 437–446 (2019).

44. Li, P. et al. Booster vaccination is required to elicit and maintain COVID-19 vaccine-induced immunity in SIV-infected macaques. *Emerg. Microbes Infect.* **12**, e2136538 (2023).

45. Darrah, P. A. et al. Airway T cells are a correlate of i.v. bacille Calmette–Guerin-mediated protection against tuberculosis in rhesus macaques. *Cell Host Microbe* https://doi.org/10.1016/j.chom.2023.05.006 (2023).

46. Gideon, H. P. et al. Multimodal profiling of lung granulomas in macaques reveals cellular correlates of tuberculosis control. *Immunity* **55**, 827–846.e810 (2022).

47. Lu, L. L. et al. A functional role for antibodies in tuberculosis. *Cell* **167**, 433–443 e414 (2016).

48. Gasper, M. A. et al. BCG vaccination induces HIV target cell activation in HIV-exposed infants in a randomized trial. *JCI Insight* **2**, e91963 (2017).

49. Wood, M. P. et al. Transient immune activation in BCG-vaccinated infant rhesus macaques is not sufficient to influence oral simian immunodeficiency virus infection. *J. Infect. Dis.* **222**, 44–53 (2020).

50. Lu, J. et al. Expansion of circulating T follicular helper cells is associated with disease progression in HIV-infected individuals. *J. Infect. Public Health* **11**, 685–690 (2018).

51. Petrovas, C. et al. CD4 T follicular helper cell dynamics during SIV infection. *J. Clin. Invest.* **122**, 3281–3294 (2012).

52. Shen, Y. et al. Induction of an AIDS virus-related tuberculosis-like disease in macaques: a model of simian immunodeficiency virus-mycobacterium coinfection. *Infect. Immun.* **70**, 869–877 (2002).

53. Cirovic, B. et al. BCG Vaccination in humans elicits trained immunity via the hematopoietic progenitor compartment. *Cell Host Microbe* **28**, 322–334.e325 (2020).

54. Vierboom, M. P. M. et al. Stronger induction of trained immunity by mucosal BCG or MTBVAC vaccination compared to standard intradermal vaccination. *Cell Rep. Med.* **2**, 100185 (2021).

55. van Puffelen, J. H. et al. Intravesical BCG in patients with non-muscle invasive bladder cancer induces trained immunity and decreases respiratory infections. *J. Immunother. Cancer* **11**, e005518 (2023).

56. Kaufmann, E. et al. BCG educates hematopoietic stem cells to generate protective innate immunity against tuberculosis. *Cell* **172**, 176–190.e119 (2018).

57. Kleinnijenhuis, J. et al. Bacille Calmette–Guerin induces NOD2-dependent nonspecific protection from reinfection via epigenetic reprogramming of monocytes. *Proc. Natl Acad. Sci. USA* **109**, 17537–17542 (2012).

58. Kleinnijenhuis, J. et al. Long-lasting effects of BCG vaccination on both heterologous Th1/Th17 responses and innate trained immunity. *J. Innate Immun.* **6**, 152–158 (2014).

59. Dellagostin, O. A., Borsuk, S., Oliveira, T. L. & Seixas, F. K. Auxotrophic *Mycobacterium bovis* BCG: updates and perspectives. *Vaccines* **10**, 802 (2022).

60. Verreck, F. A. W. et al. Variable BCG efficacy in rhesus populations: pulmonary BCG provides protection where standard intra-dermal vaccination fails. *Tuberculosis* **104**, 46–57 (2017).

61. Dijkman, K. et al. Pulmonary MTBVAC vaccination induces immune signatures previously correlated with prevention of tuberculosis infection. *Cell Rep. Med.* **2**, 100187 (2021).

62. Budde, M. L. et al. Characterization of Mauritian cynomolgus macaque major histocompatibility complex class I haplotypes by high-resolution pyrosequencing. *Immunogenetics* **62**, 773–780 (2010).

63. Wiseman, R. W. et al. Simian immunodeficiency virus SIVmac239 infection of major histocompatibility complex-identical cynomolgus macaques from Mauritius. *J. Virol.* **81**, 349–361 (2007).

64. Ellis-Connell, A. L. et al. Control of simian immunodeficiency virus infection in prophylactically vaccinated, antiretroviral treatment-naive macaques is required for the most efficacious CD8 T cell response during treatment with the interleukin-15 superagonist N-803. *J. Virol.* **96**, e0118522 (2022).

65. Ben Youssef, G. et al. Ontogeny of human mucosal-associated invariant T cells and related T cell subsets. *J. Exp. Med.* **215**, 459–479 (2018).

66. Hartman, A. L. et al. SARS-CoV-2 infection of African green monkeys results in mild respiratory disease discernible by PET/CT imaging and shedding of infectious virus from both respiratory and gastrointestinal tracts. *PLoS Pathog.* **16**, e1008903 (2020).

67. Sarnyai, Z. et al. Performance evaluation of a high-resolution nonhuman primate PET/CT system. *J. Nucl. Med.* **60**, 1818–1824 (2019).

68. White, A. G. et al. Analysis of [18]FDG PET/CT imaging as a tool for studying *Mycobacterium tuberculosis* infection and treatment in non-human primates. *J. Vis. Exp.* https://doi.org/10.3791/56375 (2017).

Author contributions

C.A.S. and S.L.O. obtained funding for this study. C.A.S. and S.L.O. conceived and designed the experiments with J.L.F., R.A.S. and M.R. All animal protocols and experiments were coordinated by C.A.S. at the University of Pittsburgh. Animal care and procedures were performed by J.A.T. and K.B.K. Flow cytometry panels used to assess immunology were designed by E.C.L., A.L.E.-C. and P.A.D. and flow cytometry was performed by E.C.L., A.N.B. and S.J. Antibody ELISAs and plasma viral loads were performed by A.L.E.-C. and R.V.M., respectively, at the University of Wisconsin – Madison. M.A.R., A.K.G., J.L.G. and C.L.A. processed NHP samples and CFU. J.A.T., P.M., H.J.B. and A.G.W. performed PET/CT scans and image analyses. E.K. and P.L.L. performed the necropsies. E.K. assessed TB pathology. E.C.L., A.L.E.-C., A.J.B., M.A.R. and P.M. performed the data analysis and generated figures. P.M. provided statistical guidance for all figures. E.C.L. wrote the manuscript with help from C.A.S., J.L.F., S.L.O., A.L.E.-C., P.A.D., P.L.L. and P.M.

Competing interests

The authors declare no competing interests.

Additional information

Extended data is available for this paper at https://doi.org/10.1038/s41564-023-01503-x.

Supplementary information The online version contains supplementary material available at https://doi.org/10.1038/s41564-023-01503-x.

Correspondence and requests for materials should be addressed to Erica C. Larson.
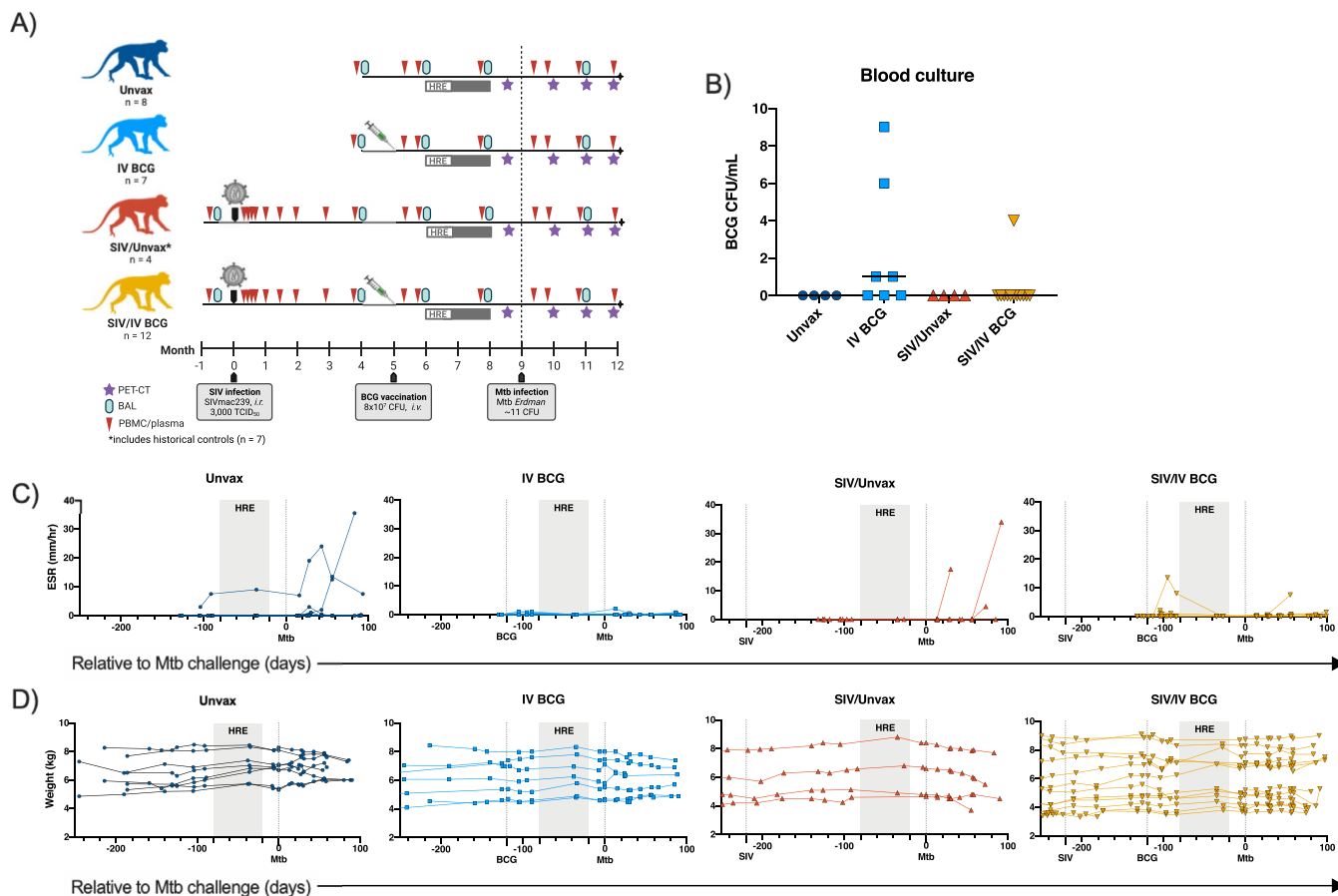
Peer review information *Nature Microbiology* thanks the anonymous reviewer(s) for their contribution to the peer review of this work.

Reprints and permissions information is available at www.nature.com/reprints.

Publisher's note Springer Nature remains neutral with regard to jurisdictional claims in published maps and institutional affiliations.

Extended Data Fig. 1 | Study outline and clinical parameters. a) Timeline of NHP groups including SIV infection, BCG vaccination, HRE therapy, and Mtb challenge. Sampling schedule of blood draws, BAL, and PET-CT image is also included. Created with BioRender.com. **b)** BCG CFU/mL of blood cultures collected 2 wks after vaccination. Horizontal bars indicate group medians and symbols indicate individual animals (Unvax, n = 4; IV BCG, n = 7; SIV/Unvax, n = 4; SIV/IV BCG, n = 12). **c)** ESR (mm/hr) of individual animals in each group relative to Mtb challenge. **d)** Individual animal weights (kg) of each group relative to Mtb challenge. C & D) Symbols indicate individual animals (Unvax, n = 8; IV BCG, n = 7; SIV/Unvax, n = 4; SIV/IV BCG, n = 12).
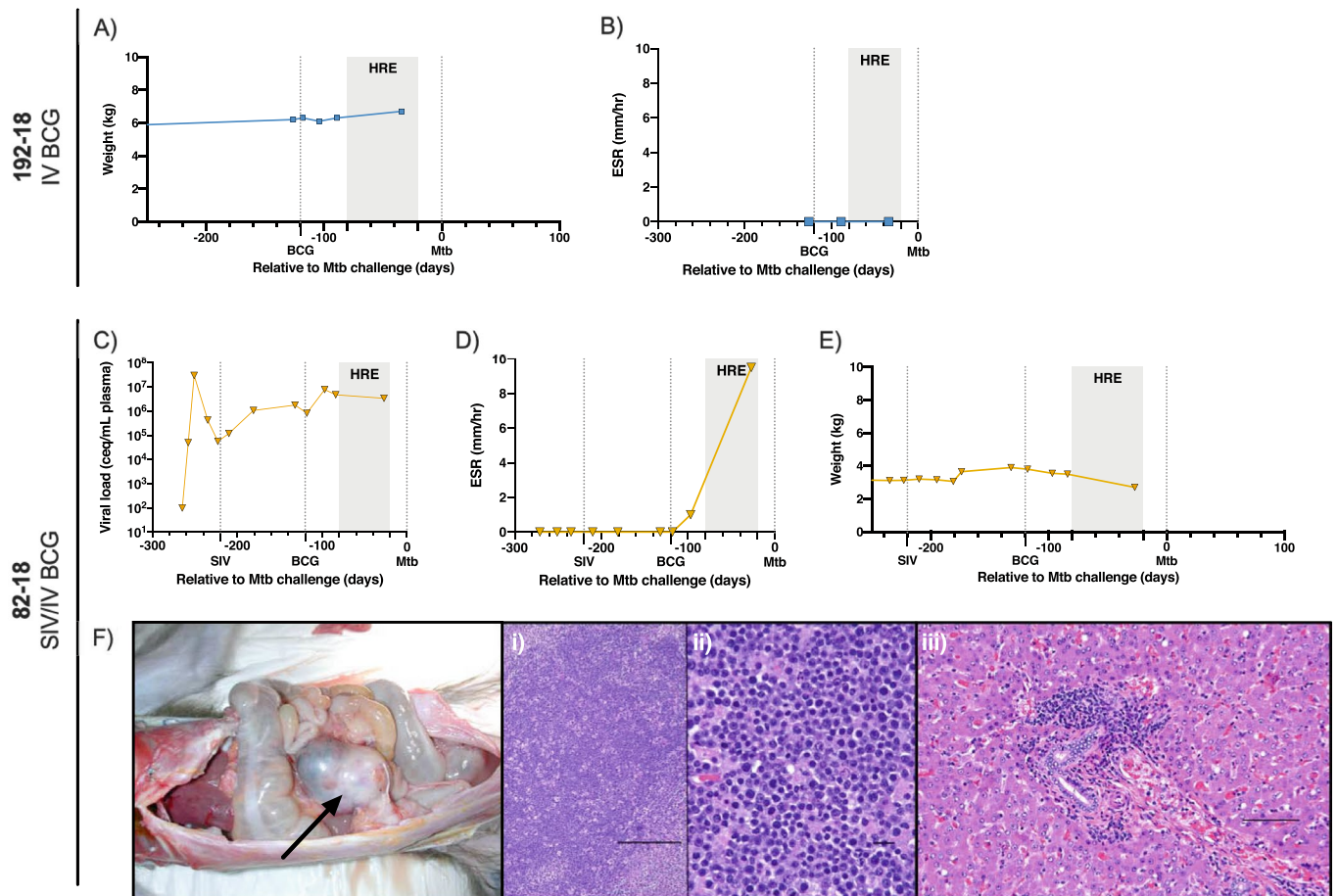
Extended Data Fig. 2 | Clinical parameters of 192-18 and 82-18. a) Weight of 192-18 over time relative to Mtb challenge. **b)** ESR of 192-18 over time. **c)** Weight of 82-18 over time relative to Mtb challenge. **d)** ESR of 82-18 over time. **e)** Plasma viral load over course of study. **f)** Histopathological signs of lymphoma in 82-18. Photomicrographs were representative of 30 slides examined per animal. Left panel: image of ileocecocolic mass (black arrow). Middle panel (i & ii): 10X (left; scale bar = 100 μm) and 40X (right; scale bar = 10 μm) H&E-stained section of ileocecocolic mass indicating large non-cleaved lymphoid population. Right panel (iii): H&E-stained section of liver (20X), peri-portal lymphoid infiltration (scale bar = 50 μm).
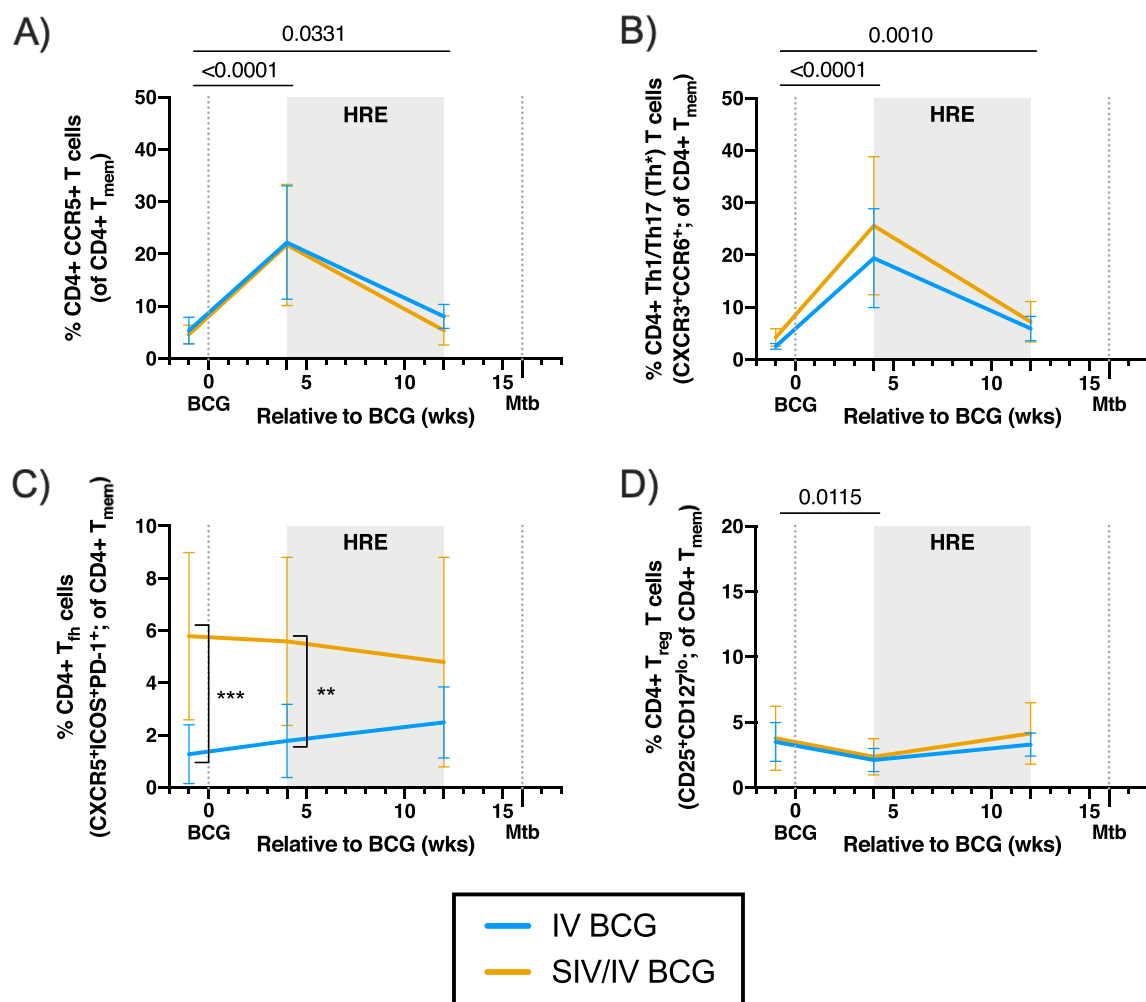
Extended Data Fig. 3 | CD4 + T cell phenotype in PBMC after vaccination.
a) Frequency of CD4 + CCR5 + T cells in PBMC relative to BCG vaccination. **b)** Frequency of CD4 + Th1/Th17 (Th*) T cells (CXCR3$^+$CCR6$^+$) in PBMC relative to BCG vaccination. **c)** Frequency of CD4+ T$_{fh}$ T cells (CXCR5$^+$ICOS$^+$PD-1$^+$) in PBMC relative to BCG vaccination. **d)** Frequency of CD4+ T$_{reg}$ T cells (CD25$^+$CD127^{lo}) in PBMC relative to BCG vaccination. **a-d)** Lines indicate mean and error bars indicate SD of SIV-naïve (light blue) and SIV+ (gold) vaccinated animals. SIV-naïve vaccinated animals: pre-BCG (n = 7), 4 wks post BCG (n = 7), and 12 wks post BCG (n = 7). SIV+ vaccinated animals: pre-BCG (n = 12), 4 wks post BCG (n = 12), and 12 wks post BCG (n = 11). Individual animal data are shown in Supplementary Data

8. Linear mixed effects models with subject as a random variable were used. Fixed effect tests were used to assess mean differences among time points and vaccine groups. Time points were compared to 'pre-BCG' control using Dunnett's multiple comparison tests. Significant p-values (p < 0.05) across time are shown above each graph. Significant differences determined by Mann-Whitney tests between vaccination groups at given time points are indicated by brackets and significant p-values indicated: **p < 0.01 and ***p < 0.001. Fixed effect test results, Dunnett's multiple comparisons, and Mann-Whitney test results are reported in Supplementary Table 2C. All statistical tests were two-sided.
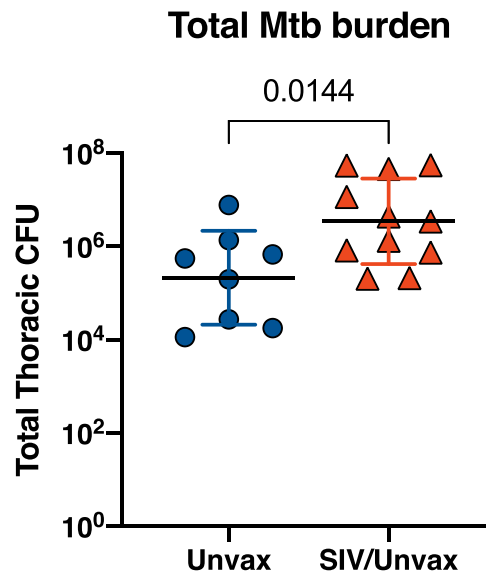
Total Mtb burden

Extended Data Fig. 4 | Bacterial burden of SIV-naïve and SIV+ unvaccinated animals. Total thoracic Mtb burden at necropsy. Each point indicates an individual animal, horizontal bars indicate group means, and error bars indicate standard deviation. Unpaired t test (two-sided) was performed between SIV-naïve unvaccinated (Unvax, dark blue circles; n = 8) and SIV+ unvaccinated groups (SIV/Unvax, red, up-pointing triangles; n = 11). P-value is shown.
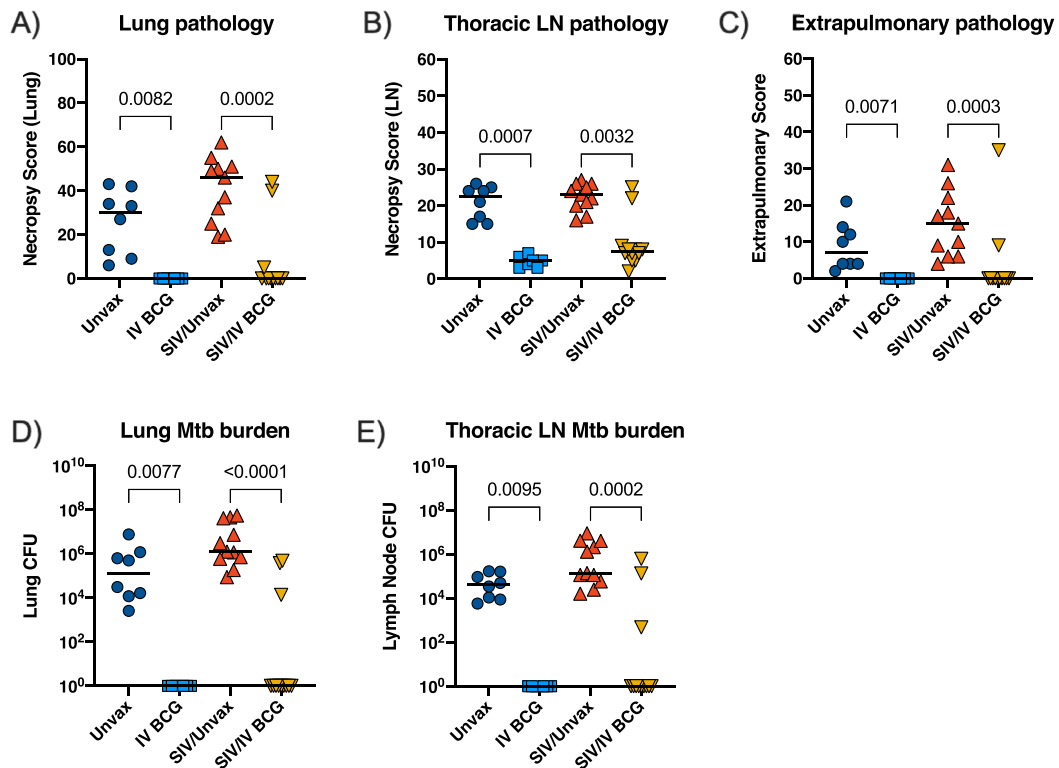
Extended Data Fig. 5 | TB outcome by tissue compartment. a-e) Lung pathology **(a)**, thoracic lymph node (LN) pathology **(b)**, extrapulmonary pathology **(c)**, lung Mtb burden **(d)**, and thoracic LN Mtb burden **(e)** at necropsy. Each point indicates an individual animal and horizontal bars indicate group medians (Unvax, n = 8; IV BCG, n = 7; SIV/Unvax, n = 11; SIV/IV BCG, n = 12).

Kruskal Wallis tests were performed with Dunn's multiple comparisons between SIV-naïve, vaccinated and unvaccinated groups (dark blue circles and light blue squares, respectively); and SIV+, vaccinated and unvaccinated groups (red, up-pointing triangle and gold, down-pointing triangle, respectively). P-values are shown. All statistical tests were two-sided.
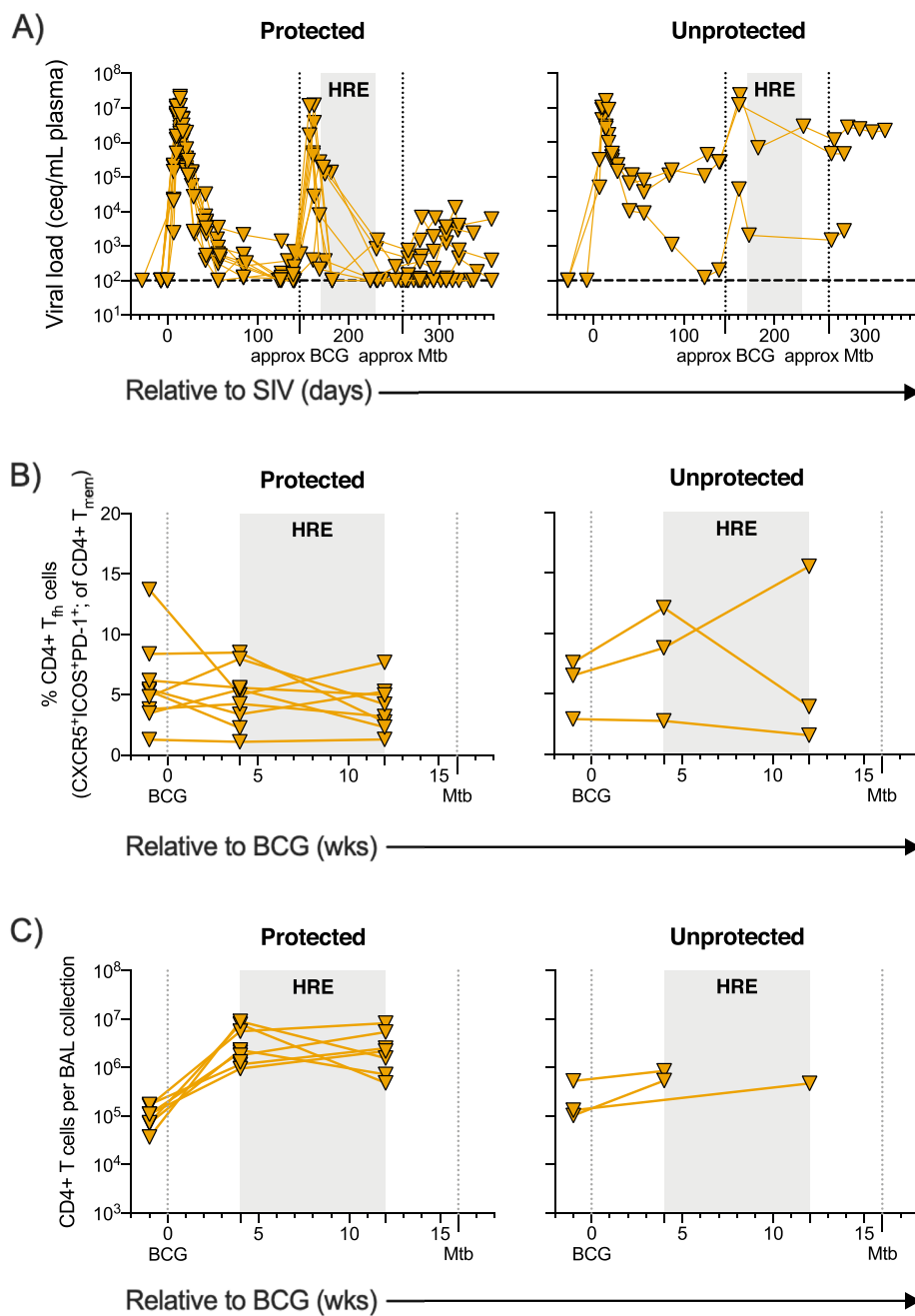
Extended Data Fig. 6 | Plasma viral load, PBMC CD4+ T$_{fh}$ T cells, and BAL CD4 + T cell levels stratified by protection across SIV+ vaccinated animals. Individual symbols and lines indicate protected animals (thoracic CFU < 100, n = 9) and unprotected animals (thoracic CFU > 100, n = 3). **a)** Plasma viremia in protected and unprotected SIV+, vaccinated animals over the course of the study.

b) Frequency of CD4+ T$_{fh}$ T cells (CXCR5$^+$ICOS$^+$PD-1$^+$) in PBMC from protected and unprotected SIV+, vaccinated animals relative to BCG vaccination. **c)** Number of CD4 + T cells per BAL collection in protected and unprotected SIV+, vaccinated animals relative to BCG vaccination.

Extended Data Table 1 | Summary of MCM and outcome measures following IV BCG vaccination and Mtb challenge

Group	NHP #	Gender	MHC Haplotype	Age	BCG dose (CFU)	Blood culture Post BCG 2 wks (CFU/mL)	Mtb dose (CFU)	Weeks to Necropsy (Post Mtb infection)	ESR (mm/hr)	GA (CFU/mL)	BAL (CFU/mL)	Gross pathology score	Total Mtb CFU
Unvax	15719	M	M1/M2	5 y 9 m	N/A	N/A	21	11.9	+ (3 @ 4 wk)	neg	+ (8 wks)	75	1.4×10^6
	15819	M	M4M1/recM3M1	6 y 3 m	N/A	N/A	21	12.1	+ (pre Mtb infection)	+ (4 wks)	+ (8 wks)	56	5.5×10^5
	15919	M	M1/M2	8 y 1 m	N/A	N/A	21	13.0	neg	neg	neg	23	1.8×10^4
	16019	M	M1/M4	6 y 3 m	N/A	N/A	21	13.3	neg	neg	neg	37	2.8×10^4
	16119	M	M1/M3	9 y 2 m	N/A	0	6	13.0	neg	neg	+ (8 wks)	69	6.7×10^5
	16419	M	M1/M6	7 y 2 m	N/A	0	6	13.3	+ (8 wks)	neg	neg	76	2.0×10^5
	16519	M	M1/recM2M5	8 y 3 m	N/A	0	4	12.6	neg	neg	N/A	64	7.7×10^6
	16719	M	M1/recM4M1	5 y 6 m	N/A	0	4	12.9	neg	neg	N/A	27	1.1×10^4
IV BCG	18918	M	M1/recM4M1	5 y 8 m	8.4×10^7	1	8	12.1	neg	neg	neg	3	0
	19018	M	M1/M5	5 y 8 m	8.4×10^7	1	8	12.4	neg	neg	neg	4	0
	19118	M	M1/M4	6 y 8 m	8.4×10^7	6	8	12.4	neg	neg	neg	6	0
	16219	M	M1/M3	9 y 2 m	6.3×10^7	0	6	13.0	neg	neg	neg	5	0
	16919	M	M1/M4	5 y 5 m	6.3×10^7	0	6	13.3	neg	neg	neg	5	0
	16619	M	M1/M3	8 y 3 m	1.0×10^6	9	4	12.6	neg	neg	N/A	5	0
	17119	M	M1/recM1M4	11 y 3 m	1.0×10^6	0	4	12.9	neg	neg	N/A	3	0
SIV/Unvax	8518	F	M1/M3	10 y 0 m	N/A	0	16	7.9	+ (17.5 @ 4 wks)	+ (4 wks)	neg	97	5.5×10^7
	8718	F	M1/M3	10 y 7 m	N/A	0	10	10.4	+ (4.5 @ 10 wks)	+ (8 wks)	+ (8 wks)	79	3.5×10^6
	9018	M	M1/M6	10 y 1 m	N/A	0	16	12.1	neg	+ (8 wks)	neg	45	2.1×10^5
	17419	M	M1/M5	5 y 7 m	N/A	0	4	13.1	neg	neg	+ (8 wks)	73	5.6×10^7
	6016	M	M1/M1	11 y 5 m	N/A	N/A	12	11.0	neg	+ (8 wks)	+ (4 wks)	56	2.1×10^5
	6416	M	M1/M1	9 y 1 m	N/A	N/A	12	9.0	+ (38.5 @ 8 wks)	+ (4 & 8 wks)	neg	114	4.6×10^7
	6716	M	M1/M2	10 y 8 m	N/A	N/A	12	11.0	neg	+ (8 wks)	neg	85	1.3×10^6
	12415	F	M1/recM3M2	7 y 9 m	N/A	N/A	6	12.0	neg	+ (8 wks)	+ (8 wks)	85	4.4×10^6
	12715	F	M1/M2	7 y 6 m	N/A	N/A	6	12.0	neg	+ (4 & 8 wks)	neg	75	7.4×10^5
	13015	M	M1/recM3M2	6 y 5 m	N/A	N/A	6	13.0	neg	+ (4 & 8 wks)	+ (8 wks)	54	8.3×10^5
	13115	M	M1/recM1M2	7 y 4 m	N/A	N/A	6	9.0	neg	+ (4 & 8 wks)	neg	62	1.2×10^7
SIV/IV BCG	8318	F	M1/M3	8 y 11 m	8.1×10^7	0	10	11.0	neg	+ (4 wks)	neg	26	0
	8618	F	M1/M3	10 y 8 m	8.1×10^7	0	16	11.9	neg	neg	neg	2	0
	8818	F	M1/M3	10 y 2 m	8.1×10^7	0	10	11.0	neg	neg	+ (4 wks)	8	0
	19318	M	M1/M2	5 y 10 m	8.7×10^7	0	18	13.1	neg	neg	neg	5	0
	19418	M	M1/recM4M2	4 y 10 m	8.7×10^7	0	18	13.1	neg	neg	neg	5	0
	19518	M	M1/recM4M2	5 y 9 m	8.7×10^7	4	18	11.4	+ (7.5 @ 8 wks)	+ (8 wks)	neg	88	6.3×10^5
	19618	M	M1/recM1M3M4	4 y 10 m	8.7×10^7	0	18	13.4	neg	neg	neg	7	0
	17019	M	M1/recM3M4	7 y 7 m	5.0×10^7	0	4	14.1	neg	+ (8 wks)	neg	71	1.1×10^6
	17219	M	M1/M2	8 y 7 m	5.0×10^7	0	4	14.1	neg	neg	neg	3	0
	17319	M	M1/M6	13 y 7 m	5.0×10^7	0	4	13.1	neg	neg	neg	13	1.4×10^4
	16319	M	M1/M4	7 y 2 m	2.1×10^7	0	14	12.3	+ (0.75 @ 8 wks)	neg	neg	7	0
	17519	M	M1/M1	10 y 10 m	2.1×10^7	0	14	12.3	+ (0.5 @ 12 wks)	neg	neg	8	0
Animals excluded from analysis	8218	F	M1/M3	8 y 11 m	8.1×10^7	0	N/A	N/A	+ (9.5 @ 12 wks post BCG)	N/A	N/A	N/A	0 (BCG CFU)
	19218	M	M1/M4	6 y 4 m	8.4×10^7	0	N/A	N/A	N/A	N/A	N/A	N/A	N/A

Historical controls in the SIV/Unvax group include: 6016, 6416, 6716, 12415, 12715, 13015, and 13115. Age is indicated as years (y) and months (m). For ESR, GA, and BAL, time point indicated post Mtb infection, unless otherwise stated. Total Mtb CFU limit of detection (LOD) is < 100 CFU per animal. One haplotype from 15819 expressed the M3 class I A alleles, but M1 class I B and II alleles - the M3 and M1 class I A regions share the major MHC class I A allele Mafa-A1*063, but the signal peptide sequence differs by one amino acid between the two haplotypes[54]. The recombinant haplotype of 171-19 contains M1 MHC class I A alleles and M4 MHC class I B and class II alleles. The recombinant haplotype of 131-15 contains M1 MHC class I B alleles and M2 MHC class I A and class II alleles.

nature portfolio

Corresponding author(s):   Drs. Erica Larson and Charles Scanga

Last updated by author(s):   Sep 6, 2023

Reporting Summary

Nature Portfolio wishes to improve the reproducibility of the work that we publish. This form provides structure for consistency and transparency in reporting. For further information on Nature Portfolio policies, see our Editorial Policies and the Editorial Policy Checklist.

Statistics

For all statistical analyses, confirm that the following items are present in the figure legend, table legend, main text, or Methods section.

n/a	Confirmed	
☐	☒	The exact sample size (*n*) for each experimental group/condition, given as a discrete number and unit of measurement
☐	☒	A statement on whether measurements were taken from distinct samples or whether the same sample was measured repeatedly
☐	☒	The statistical test(s) used AND whether they are one- or two-sided *Only common tests should be described solely by name; describe more complex techniques in the Methods section.*
☒	☐	A description of all covariates tested
☐	☒	A description of any assumptions or corrections, such as tests of normality and adjustment for multiple comparisons
☐	☒	A full description of the statistical parameters including central tendency (e.g. means) or other basic estimates (e.g. regression coefficient) AND variation (e.g. standard deviation) or associated estimates of uncertainty (e.g. confidence intervals)
☐	☒	For null hypothesis testing, the test statistic (e.g. *F*, *t*, *r*) with confidence intervals, effect sizes, degrees of freedom and *P* value noted *Give P values as exact values whenever suitable.*
☒	☐	For Bayesian analysis, information on the choice of priors and Markov chain Monte Carlo settings
☒	☐	For hierarchical and complex designs, identification of the appropriate level for tests and full reporting of outcomes
☒	☐	Estimates of effect sizes (e.g. Cohen's *d*, Pearson's *r*), indicating how they were calculated

Our web collection on statistics for biologists contains articles on many of the points above.

Software and code

Policy information about availability of computer code

Data collection	SpectroFlo v2.2; FACS Diva v9.3; ImmunoSpot software v5.1; Promega GloMax Multi detection system software v1.3.2; Roche LightCycler 480 software v1.5; OsiriX MD software v12.5.2.
Data analysis	FlowJo v10.1 & v10.8.1; Prism v8.2.1

For manuscripts utilizing custom algorithms or software that are central to the research but not yet described in published literature, software must be made available to editors and reviewers. We strongly encourage code deposition in a community repository (e.g. GitHub). See the Nature Portfolio guidelines for submitting code & software for further information.

Data

Policy information about availability of data

All manuscripts must include a data availability statement. This statement should provide the following information, where applicable:
- Accession codes, unique identifiers, or web links for publicly available datasets
- A description of any restrictions on data availability
- For clinical datasets or third party data, please ensure that the statement adheres to our policy

All relevant data are available from the corresponding author upon reasonable request.

Research involving human participants, their data, or biological material

Policy information about studies with human participants or human data. See also policy information about sex, gender (identity/presentation), and sexual orientation and race, ethnicity and racism.

Reporting on sex and gender	N/A
Reporting on race, ethnicity, or other socially relevant groupings	N/A
Population characteristics	N/A
Recruitment	N/A
Ethics oversight	N/A

Note that full information on the approval of the study protocol must also be provided in the manuscript.

Field-specific reporting

Please select the one below that is the best fit for your research. If you are not sure, read the appropriate sections before making your selection.

☒ Life sciences   ☐ Behavioural & social sciences   ☐ Ecological, evolutionary & environmental sciences

For a reference copy of the document with all sections, see nature.com/documents/nr-reporting-summary-flat.pdf

Life sciences study design

All studies must disclose on these points even when the disclosure is negative.

Sample size	We used total thoracic bacterial burden (log10) as the primary outcome variable with a pooled standard deviation of 1.09 (calculated by averaging standard deviations of all groups) for a two-sided test and adjusted the type I error for two comparisons (alpha = 0.025). For the unvaccinated (n = 8) and IV BCG (n = 7) comparison, we obtained 83.0% power to detect a mean difference of 2 in bacterial burden. For the SIV/Unvaccinated (n = 11) and SIV/IV BCG (n = 12) comparison, we obtained 97.0% power to detect a mean difference of 2.
Data exclusions	Two IV BCG-vaccinated animals (82-18 & 192-18) did not reach Mtb challenge due to reasons unrelated to BCG. For this reason, we were unable to assess vaccine efficacy and related immune parameters and these animals were excluded from all analyses. For BAL analyses, some time points either did not have enough cells for all tests in which they were prioritized for ICS, had low cell viability (< 70%), or displayed autofluorescence that reduced the signal to noise ratio rendering gating positive populations difficult. For these reasons, these data were excluded from BAL analyses.
Replication	Due to limitations of NHP studies (i.e., cost and animal welfare), we conducted a power analysis to detect a meaningful effect size.
Randomization	Animals were arbitrarily assigned to groups.
Blinding	Technicians that performed qPCR for plasma viral loads were blinded from treatment group. Prosectors who conducted the necropsies, image analysts for PET/CT, the pathologist and technicians who processed samples were blinded from treatment group as well. Flow cytometry and Antibody ELISA analyses was performed by investigators (E.C.L., A.L.E.C., & A.J.B.) who were intimately familiar with all aspects of the study including group assignments which made it impossible to blind.

Reporting for specific materials, systems and methods

We require information from authors about some types of materials, experimental systems and methods used in many studies. Here, indicate whether each material, system or method listed is relevant to your study. If you are not sure if a list item applies to your research, read the appropriate section before selecting a response.

Materials & experimental systems

n/a	Involved in the study
☐	☒ Antibodies
☒	☐ Eukaryotic cell lines
☒	☐ Palaeontology and archaeology
☐	☒ Animals and other organisms
☒	☐ Clinical data
☒	☐ Dual use research of concern
☒	☐ Plants

Methods

n/a	Involved in the study
☒	☐ ChIP-seq
☐	☒ Flow cytometry
☒	☐ MRI-based neuroimaging

Antibodies

Antibodies used

Flow cytometry:
PBMC ICS
CD107a BUV395 (BD; Cat No. 565113; Clone eBioH4A3; dilution: 1:25) and CD154 BV421 (BD; Cat No. 563886; Clone TRAP1; dilution: 1:25) was added during the BFA and monensin step 2 hours after the stimulators were added. After the 14-hour stimulation, cells were stained for viability using LIVE/DEAD™ Fixable Blue Dead Cell Stain Kit (Invitrogen; Cat No. L23105; dilution: 1:1000). For the surface antibody cocktail, the following antibodies were used: Vg9 FITC (Invitrogen; Cat No. TCR2720; Clone 7A5; dilution: 1:40); CCR4 BV510 (Biolegend; Cat No. 359416; Clone L291H4; dilution: 1:50); CXCR3 BV605 (Biolegend; Cat No. 353728; Clone G025H7; dilution: 1:20); PD-1 BV711 (Biolegend; Cat No. 329928; Clone EH12.2H7; dilution: 1:20); CD4 BUV496 (BD; Cat No. 750591; Clone L200; dilution: 1:400); CCR6 BUV737 (BD; Cat No. 612780; Clone 11A9; dilution: 1:25); CD8 BUV805 (BD; Cat No. 564912; Clone SK1; dilution: 1:40); CCR7 Alexa Fluor 700 (BD; Cat No. 561143; Clone 150503; dilution: 1:20); CD3 APC-Cy7 (BD; Cat No. 557757; Clone SP34-2; dilution: 1:200); CD28 PE-Cy5 (BD; Cat No. 555730; Clone CD28.2; dilution: 1:20); and CD45RA PE-Cy7 (BD; Cat No. 561216; Clone 5H9; dilution: 1:160). For the intracellular antibody cocktail, the following antibodies were used: IL-17A BV570 (Biolegend; Cat No. 512324; Clone BL168; dilution: 1:25; TNF BV650 (BD; Cat No. 563418; Clone MAb11; dilution: 1:20); IL-2 BV750 (BD; Cat No. 566361; Clone MQ1-17H12; dilution: 1:50); IFNg APC (BD; Cat No. 554702; Clone B27; dilution: 1:200); CD69 ECD (Beckman; Cat No. 6607110; Clone TP1.55.3; dilution: 1:100); Granulysin PE (Biolegend; Cat No. 348004; Clone DH2; dilution: 1:20); and Granzyme B PE-Cy5.5 (Invitrogen; Cat No. GRB18; Clone GB11; dilution: 1:160). All samples were stained in a final volume of 50 uL.

PBMC Phenotype
Cells were with MR-1 tetramer BV421 loaded with 5-OPRU (NIH Tetramer Core; dilution: 1:50) for 30 minutes at 4C. Viability was subsequently stained using LIVE/DEAD™ Fixable Blue Dead Cell Stain Kit (Invitrogen; Cat No. L23105; dilution: 1:1000). For the surface antibody cocktail, the following antibodies were used: Vg9 FITC (Invitrogen; Cat No. TCR2720; Clone 7A5; dilution: 1:40); PD-1 BB660 (BD; custom order; clone EH12.1; dilution: 1:50); CCR7 BB700 (BD; Cat No. 566437; Clone 3D12; dilution 1:20); CD127 BV510 (Biolegend; Cat No. 351332; Clone A019D5; dilution: 1:40); CD20 BV570 (Biolegend; Cat No. 302331; Clone 2H7; dilution: 1:40); CXCR5 Super Bright 600 (Invitrogen; Cat No. 63-9185-42; Clone MU5UBEE; dilution: 1:10); CD16 BV650 (BD; Cat No. 563692; Clone 3G8; dilution: 1:80); CXCR3 BV711 (Biolegend; Cat No. 353732; Clone G025H7; dilution 1:10); CD14 BV785 (Biolegend; Cat No. 301839; Clone M5E2; dilution 1:80); CD45RA BUV395 (BD; Cat No. 740315; Clone 5H9; dilution: 1:320); CD4 BUV496 (BD; Cat No. 750591; Clone L200; dilution: 1:400); CD25 BUV563 (BD; Cat No. 612918; Clone 2A3; dilution: 1:40); CCR6 BUV737 (BD; Cat No. 612780; Clone 11A9; dilution: 1:25); CD8 BUV805 (BD; Cat No. 564912; Clone SK1; dilution: 1:40); CCR5 APC (BD; Cat No. 564912; Clone 3A9; dilution: 1:10); ICOS R718 (BD; Cat No. 566990; Clone C398.4A; dilution: 1:160); CD3 APC-Cy7 (BD; Cat No. 557757; Clone SP34-2; dilution: 1:50); gd TCR PE (ThermoFisher; Cat No. MHGD04; Clone 5A6.E9; dilution: 1:10); NKG2a ECD (Beckman; Cat No. IM99512; Clone Z199; dilution: 1:40); CD123 PE-Cy5 (Biolegend; Cat No. 306008; Clone 6H6; dilution: 1:160); HLA-DR PE-Cy5.5 (Life Tech; Cat No. MHLDR18; Clone TU36; dilution: 1:400); and CD11c PE-Cy7 (Biolegend; Cat No. 301608; Clone 3.9; dilution: 1:100). All samples were stained in a final volume of 50 uL.

BAL ICS
CD107a PerCP-eFluor710 (eBioscience; Cat No. 46-1079-42; Clone eBioH4A3; dilution: 1:100) was added during the BFA and monensin step 2 hours after the stimulators were added. After the 14-hour stimulation, cells were washed and stained with MR-1 tetramer BV421 loaded with 5-OPRU (NIH Tetramer Core; dilution: 1:50) for 30 minutes at 4C. Viability was subsequently stained using Zombie NIR™ Fixable Viability Kit (Biolegend; Cat No. 423106; dilution 1:200). For the surface antibody cocktail, the following antibodies were used: CXCR5 Super Bright 436 (eBioscience; Cat No. 62-9185-42; Clone MU5UBEE; dilution: 1:33); CD8 Pacific Blue (Dako; Cat No. PB984; Clone DK25; dilution: 1:33); CCR7 BV480 (BD; Cat No. 566099; Clone 3D12; dilution: 1:40); CD45 BV510 (BD; Cat No. 563530; Clone DO58-1283; dilution: 1:66); PD-1 BV605 (Biolegend; Cat No. 329924; Clone EH12.2H7; dilution 1:33); CXCR3 BV711 (Biolegend; Cat No. 353732; Clone G025H7; dilution 1:33); CD127 BV785 (Biolegend; Cat No. 351330; Clone A019D5; dilution: 1:20); CD25 BB515 (BD; Cat No. 564467; Clone 2A3; dilution 1:33); Vg9 FITC (Invitrogen; Cat No. TCR2720; Clone 7A5; dilution 1:66); CD28 PE-Cy5 (BD; Cat No. 555730; Clone CD28.2; dilution 1:20); CCR6 PerCP-Cy5.5 (BD; Cat No. 560467; Clone 11A9; dilution 1:25); CD45RA PE-Cy7 (BD; Cat No. 561216; Clone 5H9; dilution 1:25); ICOS Alexa Fluor 647 (Biolegend; Cat No. 313516; Clone C398.4A; dilution 1:33); CD103 conjugated to Alexa Fluor 680 (Beckman Coulter; Cat No. IM0318; Clone 2G5; dilution 1:166); and CD4 Alexa Fluor 700 (eBioscience; Cat No. 56-0048-41; Clone OKT4; dilution 1:200). For the intracellular antibody cocktail, the following antibodies were used: IL-17A BV570 (Biolegend; Cat No. 512324; Clone BL168; dilution 1:25); TNF BV650 (Biolegend; Cat No. 502937; Clone MAb11; dilution 1:40); IL-2 PE (Biolegend; Cat No. 500307; Clone MQ1-17H12; dilution 1:33); CD69 PE-Dazzle594 (Biolegend; Cat No. 310942; Clone FN50; dilution 1:25); IFNg APC (BD; Cat No. 562017; Clone B27; dilution 1:66); and CD3 APC-Cy7 (BD; Cat No. 557757; Clone SP34-2; dilution 1:25). All samples were stained in a final volume of 100 uL for surface and intracellular antibody cocktails.

BAL Phenotype
Cells were with MR-1 tetramer BV421 loaded with 5-OPRU (NIH Tetramer Core; dilution: 1:50) for 30 minutes at 4C. Viability was subsequently stained using Zombie NIR ™ Fixable Viability Kit (Biolegend; Cat No. 423106; dilution 1:200). For the surface antibody cocktail, the following antibodies were used: CD16 Super Bright 436 (eBioscience; Cat No. 62-0166-41; Clone 3G8; dilution 1:33); CD8

Pacific Blue (Dako; Cat No. PB984; Clone DK25; dilution: 1:33); CCR7 BV480 (BD; Cat No. 566099; Clone 3D12; dilution: 1:40); CD45 BV510 (BD; Cat No. 563530; Clone DO58-1283; dilution: 1:66); CD20 BV570 (Biolegend; Cat No. 302331; Clone 2H7; dilution 1:66); PD-1 BV605 (Biolegend; Cat No. 329924; Clone EH12.2H7; dilution 1:33); CXCR3 BV711 (Biolegend; Cat No. 353732; Clone G025H7; dilution 1:33); CD14 BV785 (Biolegend; Cat No. 301839; Clone M5E2; dilution 1:25); CCR5 BB515 (BD; Cat No. 564512; Clone 3A9; dilution 1:33); Vg9 FITC (Invitrogen; Cat No. TCR2720; Clone 7A5; dilution 1:66); CD66abce PE (Miltenyi; Cat No. 130-117-811; Clone TET2; dilution 1:66); CD69 PE-Dazzle594 (Biolegend; Cat No. 310942; Clone FN50; dilution 1:25); CD11b PE-Cy5 (Biolegend; Cat No. 301307; Clone ICRF44; dilution 1:25); CD11c PE-Cy7 (Biolegend; Cat No. 301607; Clone 3.9; dilution: 1:100); NKG2a APC (Beckman; Cat No. A60797; Clone Z199; dilution 1:66); CCR4 Alexa Fluor 647 (BD; Cat No. 557863; Clone 1G1; dilution 1:50); CD4 Alexa Fluor 700 (eBioscience; Cat No. 56-0048-41; Clone OKT4; dilution 1:200); and CD163 APC-Cy7 (Biolegend; Cat No. 333622; Clone GH1-61; dilution 1:66). All samples were stained in a final volume of 100 uL.

Antibody ELISAs
The following antibodies and their final concentrations were used for ELISAs: goat anti-Monkey IgG heavy and light chain antibody – HRP conjugated (Bethyl Laboratories; Cat No. A140-102P; 50 ng/mL); goat anti-Monkey IgA (a chain) antibody – HRP conjugated (Rockland Immunochemicals Inc.; Cat No. 617-103-006; 0.1 ug/mL); and goat anti-Monkey IgM (a chain) antibody – HRP conjugated (Sera Care; Cat No. 5220-0334; 0.4 ug/mL).

All reagents are commercially available with the exception of goat anti-Monkey IgA and goat anti-Monkey IgM, which have since been discontinued. We are using alternative antibodies for current studies to detect IgA and IgM antibodies, which are comparable. Vendor information for these reagents are available upon request.

Validation

All antibodies for flow cytometry are extensively validated by the vendors and further validated by the investigators of this study.
BD website: https://www.bdbiosciences.com/en-us/products/reagents/flow-cytometry-reagents/research-reagents
Biolegend website: https://www.biolegend.com/en-us/quality
Invitrogen website: https://www.thermofisher.com/us/en/home/life-science/cell-analysis/flow-cytometry/antibodies-for-flow-cytometry.html
Beckman website: https://www.beckman.com/reagents/coulter-flow-cytometry
Miltenyi website:https://www.miltenyibiotec.com/US-en/products/macs-antibodies/antibodies-for-flow-cytometry.html

For panel design and optimization, single color controls were initially used to obtain the optimal signal to noise. Due to the overlap between humans and NHPs, clone compatibility was referenced according to the reactivity database on the NHP Reagent Resource website (https://www.nhpreagents.org/ReactivityDatabase), a reagent database that is composed of over 20 years of research contributed data. Antibody titration was performed using NHP PBMC starting with the vendor's recommended concentration and then titrating down the amount of antibody to the concentrations listed. Fluorescence minus one experiments were used to further optimize signal to noise and minimize interactions between antibody-linked fluorochromes.

Antibodies for used for ELISAs were validated previously in Darrah et al. 2020 and further optimized in the O'Connor Lab.

Animals and other research organisms

Policy information about studies involving animals; ARRIVE guidelines recommended for reporting animal research, and Sex and Gender in Research

Laboratory animals

Adult Mauritian cynomolgus macaques (Macaca fascicularis; age > 4 years old) were purchased from Bioculture US (Immokalee, FL).

Wild animals

No wild animals were used in the study.

Reporting on sex

A total of 40 animals were used for this study. Of those, 33 were contemporaneous and 7 were historical controls. We used both male and female animals, although their distribution was unequal. Of the contemporaneous animals, only 6 were female; of the historical controls, only 2 were female. The reason for this sex imbalance was supply and demand- Bioculture simply had more male animals available. Nonetheless, we have no reason to suspect that the findings reported here apply only to males. Indeed, there was no discernable effect of sex on our findings. Importantly, Extended Data Table 1 lists each animal and, among other information, indicates whether each was male or female.

Field-collected samples

No field collected samples were used in the study.

Ethics oversight

Animal protocols and procedures were approved by the University of Pittsburgh Institutional Animal Care and Use Committee (IACUC) which adheres to guidelines established in the Animal Welfare Act and the Guide for the Care and Use of Laboratory Animals, as well as the Weatherall Report (8th Edition). The University is fully accredited by AAALAC (accreditation number 000496), and its OLAW animal welfare assurance number is D16-00118. The IACUC reviewed and approved the study protocols 15035407 and 18032418, under Assurance Number A3187-01 and D16-00118, respectively.

Note that full information on the approval of the study protocol must also be provided in the manuscript.

Flow Cytometry

Plots

Confirm that:

☒ The axis labels state the marker and fluorochrome used (e.g. CD4-FITC).

☒ The axis scales are clearly visible. Include numbers along axes only for bottom left plot of group (a 'group' is an analysis of identical markers).

☒ All plots are contour plots with outliers or pseudocolor plots.

☒ A numerical value for number of cells or percentage (with statistics) is provided.

Methodology

Sample preparation

PBMC were isolated from blood using Ficoll-Paque PLUS gradient separation (GE Healthcare Biosciences. Single-cell suspensions were cryopreserved in FBS containing 10% DMSO in liquid nitrogen. BAL wash fluid (4 x 10 mL washes of PBS) was pelleted and an aliquot of wash fluid (15 mL) was cryopreserved. The remaining cells were resuspended into ELISpot media (RPMI 1640, 10% heat-inactivated human albumin, 1% L-glutamine, and 1% HEPES) and counted. BAL cells were then divided into their appropriate flow cytometry assay depending on cell yield.

Longitudinal BAL and PBMC samples were stained for leukocyte composition (phenotype) or antigen-specific T cell responses. In general, BAL cells were stained immediately and PBMC were cryopreserved and batch-analyzed at the end of the study. For BAL analyses, cells were counted and aliquoted into a 96-well plate for either phenotype or intracellular cytokine responses (1 x 10^6 cells/well). In cases where total BAL cell counts were low, cells were prioritized for the 14-hour stimulation assay. For the phenotype panel, cells were reconstituted in 500 nM dasatinib in ELISpot media to improve MR-1 (5-OP-RU; BV421) tetramer staining. Cells were incubated with MR1 tetramer (NIH Tetramer Core Facility, Atlanta, GA) for 30 minutes at 4C. The MR1 technology was developed jointly by Dr. James McCluskey, Dr. Jaime Rossjohn, and Dr. David Fairlie, and the material was produced by the NIH Tetramer Core Facility as permitted to be distributed by the University of Melbourne. Cells were then washed and stained for viability (Zombie Live/Dead near IR; Invitrogen) for 10 minutes at room temperature. Cells were then washed, incubated with surface antibody cocktail for 20 minutes at 4C, and fixed with 1% paraformaldehyde for 15 minutes. For the intracellular cytokine assay, cells were aliquoted (1 x 10^6 cells/well) into either a media control well, purified protein derivative well (PPD; 20 ug/mL; AJ Vaccines), or ESAT-6/CFP-10 overlapping peptide pools (1 ug/mL each; BEI Resources). Stimulators were added and incubated for 2 hours, then brefeldin A (1 ug/mL; Biolegend; Cat No. 420601) and monensin (1 ug/mL; Biolegend; Cat No. 420701) was added for the remainder of the stimulation time (12 hours). Cells were washed and surface markers were stained similarly as described for the phenotype panel. However, after PFA fixation, cells were permeabilized with BD Cytofix/Cytoperm™ (BD; Cat No. 554714) for 10 minutes at room temperature. Intracellular markers were stained for 20 minutes at room temperature. Stained BAL cells were run within two days of staining. Flow cytometry of BAL was performed using a Cytek Aurora (BD; SpectroFlo v2.2). FCS files were analyzed using FlowJo software for Macintosh (version 10.1).

For PBMC analyses, cells were divided to be stained for phenotype or 14-hour stimulation. PBMC stimulators include: H37Rv whole cell lysate (20 ug/mL, BEI Resources) and ESAT-6/CFP-10 peptide pools (1 ug/mL each). Cell were stained as follows: cells were stained with MR-1 tetramer for 20 minutes; washed twice with PBS/BSA (0.1%); then stained with viability dye for 20 minutes; washed twice with PBS/BSA (0.1%) and incubated with human FcR blocking reagent (Miltenyi); surface markers were stained for 20 minutes and washed three times with PBS/BSA (0.1%); cells were permeabilized with BD Cytofix/Cytoperm™ (BD; Cat No. 554714) for 20 minutes and intracellular markers were stained for 30 minutes. Data was acquired on a modified BD LSR Fortessa (FACS Diva v9.3) and analyzed in FlowJo software for Macintosh (version 10.8.1).

Instrument

Cytek Aurora and BD LSR Fortessa

Software

SpectroFlo (Cytek, v2.2), FACS Diva (BD, version 9.3), FlowJo (v10.1 & v10.8.1)

Cell population abundance

We stained 1x10^6 cells for all assays, when possible. Cell population abundance is reflective of the populations present after sample collection, as these samples were not sorted for the assays described. Cell population abundance is indicated as frequencies in source data 2, 3, and 4.

Gating strategy

See Supplemental Data 5-8 for gating strategies.

For populations identified by the BAL and PBMC phenotype panels, most positive populations were clearly separated from the negative populations (> 2 decades). For MR1 5-OP-RU staining, a control tetramer (6-FP) was used to determine gate placement for the positive population. For the ICS panels, gating for cytokines were set based on unstimulated samples (media only). For markers that did not have a clearly separated population, fluorescence minus one samples (FMOs) were used to gain a general sense of the location of the positive population. Gates were drawn along the outer edge of the negative population.

☒ Tick this box to confirm that a figure exemplifying the gating strategy is provided in the Supplementary Information.